Development of a Method for Measuring Water-Stripping Resistance of Asphalt/Siliceous Aggregate Mixtures

Tinh Nguyen
Eric Byrd
Dale Bentz
Jim Seiler

U.S. DEPARTMENT OF COMMERCE
Technology Administration
National Institute of Standards
and Technology
Gaithersburg, MD 20899

Executive Summary

The main objective of this project was to develop a nondestructive, sensitive, spectroscopic method for measuring water stripping resistance at the molecular level of asphalt/siliceous aggregate mixtures exposed to water. The study consisted of three phases. Phase 1 involved the development of a technique based on Fourier transform infrared spectroscopy in the multiple internal reflection mode to quantify the water layer at the interface between an asphalt and a siliceous aggregate. Phase 2 was to develop a technique to measure the adhesion loss of an asphalt/aggregate system exposed to water environment. And Phase 3 aimed to relate the quantity of the interfacial water layer with the adhesion loss data. This final report summarizes the research in those three areas. In addition, the report also presents the results on the use of the spectroscopic technique for evaluating the effectiveness of different antistripping agents for asphalts. And finally, based on the interfacial water information, the mechanisms of stripping of an asphalt from a siliceous aggregate and of the transport of water from the environment to the asphalt/aggregate interface are presented.

1.   Development of a Technique for Quantifying the Water Layer at the Asphalt/Siliceous Aggregate Interface

A technique based on Fourier transform infrared spectroscopy in the multiple internal reflection mode (FTIR-MIR) was developed for measuring water in situ at the interface between an asphalt and a model siliceous aggregate. The theoretical basis of this technique was derived from the internal reflection theory for a two-layer model, consisting of water at the asphalt/substrate interface and that in the asphalt film within the probing depth of the FTIR-MIR technique. Experimentally, the technique required the coating of an asphalt layer of known thickness on an internal reflection element (IRE), which served as an optical guide to obtain an infrared spectrum. A water chamber was attached to the asphalt-coated IRE, and FTIR-MIR spectra were taken automatically at specified times without disturbance of the specimens. In situ water measurements for five Strategic Highway Research Program (SHRP) core asphalts (AAC-1, AAD-1, AAG-1, AAK-1, and AAM-1) on a hydrated, SiO_2-covered Si IRE, which served as the model siliceous aggregate, were carried out. The results showed that a water film of many monolayers thick has entered the interface between the five asphalts and the model siliceous substrate. Calculations were made to demonstrate that the water detected was at or near the asphalt/siliceous aggregate interface. The results have shown that the equations used for quantifying water at the asphalt/siliceous aggregate interface are valid. The technique can measure water in situ at the asphalt/siliceous interface and provide unique information on the transport properties of water through an asphalt layer attached to a substrate. The technique developed here should be useful for evaluating asphalt/siliceous aggregate mixtures in terms of 1) water susceptibility of an asphalt/aggregate mixture, 2) effectiveness of antistripping agents, 3) effects of aggregate surface contamination and environmental temperature on water stripping, and 4) water diffusion through asphalts on an aggregate.

ii

2. Measurement of Adhesion Loss of Asphalt/Siliceous Aggregate System Exposed to Water

A method based on a pneumatic adhesion tester and a porous stub was investigated for measuring the adhesion loss of five SHRP asphalts on flat soda glass and granite substrates. The porous stub allows water to reach the interface through the asphalt film thickness. This method was found suitable for measuring the bond strengths of asphalt on flat substrates before and after exposure to water. The technique is quantitative, reproducible, simple, fast, portable, and inexpensive. The adhesion of five SHRP asphalts on both glass and granite substrates decreased substantially within a short exposure. Factors affecting the difference between the adhesion loss of asphalts on glass and granite are discussed.

3. Relationship between Interfacial Water Layer and Adhesion Loss of Asphalt/Siliceous Aggregate Systems

A good correlation between the thickness of the interfacial water layer and the adhesion loss of a model polymer/siliceous substrate system was observed. General agreements were also found between the interfacial water layer and the adhesion loss of asphalts bonded to soda and granite substrates. That is, greater amount of water at the asphalt/siliceous interface corresponds to greater adhesion loss of the same system exposed to water. These results indicated that FTIR-MIR technique can be used for estimating the stripping resistance of different asphalts on a siliceous aggregate. The application of the FTIR-MIR technique for evaluating the effectiveness of four antistripping agents was carried out.

4. Mechanisms of Asphalt Stripping from a Siliceous Aggregate and of Water Transport to the Interface

Based on quantitative information of water at the asphalt/siliceous interface, the mechanisms of asphalt stripping from a siliceous aggregate and of water transport to the interface are proposed. The stripping of asphalt from a siliceous aggregate is due to the formation of a water layer many monolayers thick at the interface between an asphalt and a siliceous aggregate. The formation of the interfacial water layer is explained by the weak secondary-force bonds formed between the acidic asphalt and the acidic siliceous aggregate as compared to the bonds between water and the same substrate. Consequently, the asphalt/siliceous bonds are not hydrolytically stable and displaced by water. Basic aggregates, such as limestone, formed strong bonds (acid-base or electrostatic interactions) with acidic asphalts, which can resist the water displacement. The thickness of the interfacial water layer is increased if there is a water-sensitive (hygroscopic) film at the interface or an osmotic pressure force exists between the outside and the interface. The thick water layer observed for the five asphalt/siliceous aggregate specimens are probably due to the presence of a water-sensitive film at the asphalt/aggregate interface. This water-sensitive film is probably due to both the inward migration of water-soluble species in the asphalt and the water-soluble materials present at the interface. The transport of water to the asphalt/aggregate interface is proposed as through the tortuous pathways formed by the water dissolution of the water-soluble

species in the asphalts. For thin asphalt films, continuous pore channels allow water to reach the interface quickly, but thick films required long or repeated exposure to establish continuous pathways for water to reach the interface.

Abstract

This study aimed to develop a sensitive spectroscopic method for measuring the water stripping resistance at the molecular level of asphalt/siliceous aggregate mixtures exposed to water. The study consisted of 1) development of a technique to quantify the water layer at the interface between an asphalt and a siliceous aggregate, 2) development of a technique to measure the adhesion loss of an asphalt/aggregate system exposed to water, and 3) providing data relating the interfacial water with the adhesion loss. This final report summarizes the results of the research in these three areas. The report also presents the mechanisms on the water stripping of an asphalt from a siliceous aggregate and on the transport of water from the environment to the asphalt/aggregate interface. The results showed that FTIR-multiple internal reflection (FTIR-MIR) spectroscopy can measure the amount and thickness of the water layer at the asphalt/siliceous interface. Further, the pneumatic adhesion tester combined with a porous stub provides a suitable tool for measuring the water-induced adhesion loss of an asphalt on a flat aggregate substrate. This adhesion test is quantitative, simple, fast, portable, and inexpensive. The thickness of the water layer at the asphalt/siliceous interface correlates well with the adhesion loss of asphalt/siliceous aggregate and other organic film/siliceous systems. The results demonstrate that FTIR-MIR technique can be used for estimating the stripping resistance at the molecular level of asphalts on a siliceous aggregate. The application of this technique for evaluating the relative effectiveness of different antistripping agents is presented.

Keywords: Adhesion, aggregate, asphalt, asphalt/aggregate interface, ATR spectroscopy, bonding strength, diffusion, FTIR, in situ measurement, internal reflection spectroscopy, quantitative, siliceous aggregate, stripping, water, water susceptibility.

Table of Contents

List of Figures

INTRODUCTION

The debonding of asphalt from mineral aggregates in the presence of water (stripping) "has been observed at times ever since asphalt paving came into existence" (1). Since stripping was first recognized as a problem, many studies have been devoted to the search for a solution to this problem (2,3). Still, stripping continues to occur in many areas, particularly for asphalt on siliceous (SiO_2) aggregates. The stripping occurs on siliceous aggregates because the bonds between the SiO_2 and the organic asphalt are not hydrolytically stable (4). This means that water is likely to enter the interface and displace the asphalt from a siliceous aggregate when a asphalt/siliceous mixture is exposed to water or to high relative humidities. This problem is magnified if there are hygroscopic salts at the interface or osmotic driving forces existing between the interface and the outside. Unfortunately, water-soluble inorganic and organic salts are almost ubiquitous contaminants at the asphalt/aggregate interface, either present before the asphalt application or migrating there during exposure. The presence of a monolayer of water at the interface would probably not interfere with the adhesion of an asphalt/aggregate mixture. However, increasing the coverage of water will, at some point, affect the bonding strength of the asphalt/aggregate mixtures.

Whether asphalts fail prematurely or in the range of their expected service lives, they require large replacement costs that could probably be reduced through development of effective methods for measuring the effects of water on the stripping of asphalt from an aggregate, for effectively evaluating the water resistance of an asphalt/aggregate mixture, and for evaluating the effectiveness of antistripping agents. A major technical barrier to overcoming the problem of stripping is the lack of an effective technique for measuring the stripping resistance of an asphalt from an aggregate. If such a technique were available, it would make possible direct studies of the effects of water on the asphalt/aggregate interaction and, ultimately, predicting the stripping characteristics of an asphalt/aggregate pair in the presence of water.

The main objective of this study was to develop a sensitive, spectroscopic technique to nondestructively evaluate the water stripping resistance at the molecular level of an asphalt on a siliceous aggregate. This study consisted of three phases. Phase 1 involved the development of a nondestructive, spectroscopic technique to measure the amount and thickness of the water layer at the interface between an asphalt and a siliceous aggregate. Phase 2 was to develop a technique to measure the adhesion loss of the asphalt/aggregate mixture exposed to water. And Phase 3 aimed to relate the quantity of the interfacial water layer obtained in Phase 1 with the adhesion loss data generated in Phase 2. If a relationship between these two quantities exists, then the spectroscopic technique can be used for assessing the stripping resistance of an asphalt on a siliceous substrate. This final report summarizes the research in those three areas. In addition, this report also presents the results on the use of the spectroscopic technique for evaluating the effectiveness of different antistripping agents for asphalts. And finally, based on the interfacial water information the mechanisms of stripping of an asphalt from a siliceous aggregate and the transport of water from the environment to the asphalt/aggregate interface are presented.

1. DEVELOPMENT OF A SPECTROSCOPIC METHOD FOR MEASURING IN SITU WATER AT THE ASPHALT/MODEL SILICEOUS AGGREGATE INTERFACE

1.1. Background

In situ measurement (amount and thickness) of the water layer at the organic film/substrate interface is the subject of great interest in many industries including asphalt pavements, organic coatings, adhesives, and electronic packagings. Water and hydroxyl groups on surfaces can be studied effectively by a number of spectroscopic methods (5-7). Similarly, techniques for studying *in situ* chemical reactions at an aqueous electrolyte/electrode interface have been developed (8,9). A technique for measuring the viscosity of thin films of aqueous solutions between two closely-spaced mica or silica surfaces has been reported (10,11). However, until recent research at the National Institute of Standards and Technology (NIST), no technique has been available for measuring *in situ* water at the asphalt/siliceous substrate interface.

In situ measurement of water at the asphalt/model siliceous aggregate interface was accomplished using Fourier transform infrared (FTIR) in the multiple internal reflection mode (FTIR-MIR). FTIR-internal reflection, commonly known as FTIR-ATR (attenuated total reflection), spectroscopy is a powerful technique to provide qualitative, as well as quantitative, information on complex molecules at surfaces and interfaces. In internal reflection, the evanescent electric field (produced on total reflections at the substrate surfaces) penetrates the surface of the sample to a depth generally on the order of one wavelength of the radiation. The evanescent field, which decays exponentially with distance in the sample, interacts with the material of interest and causes an attenuation of the reflection of the propagating beam. Detection of the attenuated radiation at the exit of the substrate yields an infrared spectrum of the sample. Thus, when an asphalt-coated specimen is exposed to water, water will eventually enter the coating/substrate interfacial region and interact with the evanescent wave and be detected. This unique mode of interaction between the evanescent wave and material has made possible a large number of applications. Also new applications are being developed each year. These applications take advantage of the technique's ability to probe the near surface layers of solids and liquids. Harrick (12,13) has developed the quantitative aspects of the internal reflection spectroscopy. The quantitative capability of this technique has been verified by experimental data from a variety of applications (14-17). The uses of this technique for the studies of adsorbed species, ultrathin organic films, and single-monolayer Langmuir-Blodgett films on substrates have been reviewed (18-23).

FTIR-internal reflection spectroscopy offers a number of advantages for studying water at the organic coating/substrate interface: 1) it is sensitive toward molecular water, its dissociated OH group, and its degrees of hydrogen bonding, 2) it can be used at ambient conditions, and thus, is suitable for *in situ* measurement, 3) it detects water from the substrate side, therefore, preventing the interference of water from the environment, and 4) under proper conditions, it can be quantitative.

1.2. Theoretical Formulation for Measuring Water at the Asphalt/Model Siliceous Substrate Interface

In the previous report (24), we described an empirical approach for measuring the thickness of the water layer at the interface between an asphalt film and a SiO_2-covered silicon substrate. Recently, we have derived equations based on the theory of internal reflection spectroscopy for quantifying the water layer at the asphalt/model siliceous substrate interface. This development eliminates the need to conduct laborious experiments for establishing the infrared absorption/water concentration curve, which is required by the empirical approach. This section describes the derivation of the equations for determining the thickness and amount of the water layer at the asphalt/model siliceous aggregate.

The theoretical basis of the model for quantifying water at the asphalt/substrate interface is derived from the penetration-depth concept of internal reflection spectroscopy developed for thin and thick films (12). The physical model in which the thickness of the water layer at the asphalt/model siliceous aggregate interface is determined by the FTIR-MIR technique is illustrated in Figure 1. The substrate in this case is a silicon (Si) internal reflection element (IRE) having a refractive index greater than those of asphalt and water. The surface of the Si substrate is covered with a thin layer of silicon dioxide (SiO_2). The problem is treated as a two-layered sample model (Figure 1). The first layer consists of a water film having thickness, l, in contact with the substrate. The second layer contains the water in the asphalt that is detected by the evanescent wave.

The total water detected by the FTIR-MIR technique is the sum of the amounts in the layer at the asphalt/substrate interface and in the asphalt layer probed by the evanescent wave. Using infrared absorbance to express the amounts of water statement may be written (25)

$$A = \frac{n_2 \, \alpha_2 \, E_o^2}{n_1 \, \cos\theta} \int_0^l e^{(\frac{-2z}{d_{pw}})} dz + \frac{a_w n_3 \, \alpha_3 \, E_o^2}{n_1 \, \cos\theta} \, e^{(\frac{-2l}{d_{pw}})} \int_l^\infty e^{(\frac{-2z}{d_{pa}})} dz \qquad (1)$$

where
θ: incident angle
z: depth from the interface
E_o: amplitude of the evanescent wave at the surface
n_1: refractive index of the substrate
n_2 and α_2: refractive index and absorption coefficient of water at the asphalt/substrate interface
n_3 and α_3: refractive index and absorption coefficient of water sorbed in the asphalt
l: thickness of the water layer at the asphalt/substrate interface
d_{pw} and d_{pa}: penetration depths of the evanescent wave in water and asphalt, respectively, and
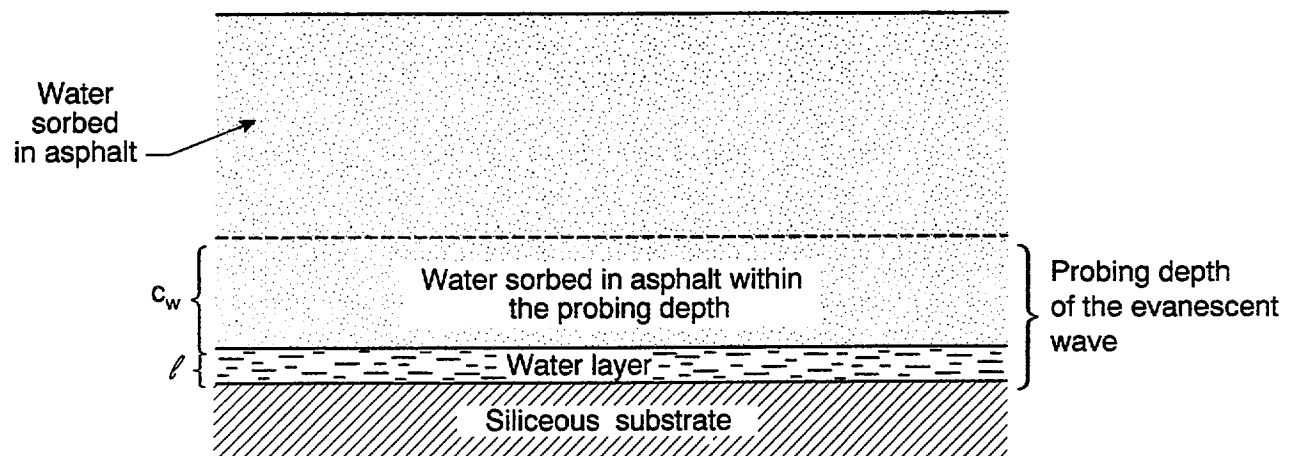a_w: fraction of water sorbed in the asphalt within the probing depth.

Figure 1. *The two-layer model used for quantifying water at the asphalt/model siliceous aggregate interface.*

The first term of Equation 1 is the absorbance (FTIR) corresponding to the amount of water at the asphalt/substrate interface. The second term represents the amount of water in the asphalt film within the probing depth of the evanescent wave. d_{pw} and d_{pc} can be obtained from (13)

$$d_p = \frac{\gamma}{2 \pi n_1 [\sin^2\theta - (\frac{n_2}{n_1})^2]^{\frac{1}{2}}}$$

(2)

where γ is the wavelength of the infrared radiation in the vacuum. d_p, commonly defined as the penetration depth of the evanescent wave, is the depth at which the amplitude of the evanescent field has decreased to $1/e$ of its value at the surface. Although the probing depth could be up to three times of d_p (15), due to the rapid decay of the evanescent wave more than 85 % of the total absorption intensity of a band is from one d_p (16,17). Thus, the majority of water detected in the asphalt-coated specimen may be assumed to be within one d_p. Equation 2 explicitly indicates that the penetration depth of the evanescent wave in the sample is a function of the angle of incidence, the wavelength of the radiation, and the refractive indices of the substrate and the sample.

Equation 2 is generally valid for non-absorbing or weakly-absorbing materials. For absorbing chemical groups, Muller et al. (26) have derived a more exact equation for d_p, which uses the complex refractive index $n_2/n_1(1+i\kappa)$ (κ is the extinction coefficient) in place of the simple refractive index n_2/n_1. Further, due to the rapid change in the magnitude of n_2 around the center of an absorption band (dispersion effect), d_p in the vicinity of the peak maximum may be different from that at or away from it, particularly for low n_1 and low θ. However, analysis by Nguyen et al. (25) has shown that the effect of absorption on d_p is negligible at the water OH stretchings band. Thus, at the band of interest (OH stretching) and for the materials used in this study Equation 2 is valid for calculating d_p.

Assuming that the refractive index and absorption coefficient of water at the asphalt/substrate interface are the same as those for water sorbed in the asphalt, i.e., $n_2 = n_3$ and $\alpha_2 = \alpha_3$ (a reasonable assumption), integrating and rearranging Equation 1 yield an expression for calculating the thickness of the water layer at the coating/substrate interface, l:

$$l = \frac{d_{pw}}{2} [-\ln \frac{1 - \frac{A}{A_\infty}}{1 - a_w \frac{d_{pa}}{d_{pw}}}]$$

(3)

where

$$A_\infty = \frac{n_2 \, \alpha_2 \, E_o^2 \, d_{pw}}{2 \, n_1 \, \cos\theta}$$

(4)

5

and A_∞ is the infrared absorbance when the water layer at the asphalt/substrate interface is very thick ($l\to\infty$, i.e., $l > d_{pw}$). Physically, this means that the water layer at the interface is so thick that the amplitude of the evanescent wave decays to a negligible value within it. In this instance, only the first term of Equation 1 remains. Equation 3 is still valid for the case where the water layer at the asphalt/substrate interface is not continuous, e.g., discrete droplets, provided that the height of the droplet is not greater than the probing depth of the evanescent wave in water. Reference 25 gives detailed derivation of Equation 3 from Equation 2.

Assuming water is uniformly distributed over the entire surface area of the specimen, the amount of water at the asphalt/substrate interface, Q_i, will be given by

$$Q_i = l\,a\,\rho \tag{5}$$

where l is the thickness of the water layer, a is the area of the asphalt specimen in contact with water, and ρ is the density of water at the interface.

To obtain the thickness l and amount Q_i of water at the interface using Equations 3 and 5, A, A_∞, a_w, d_{pc} and d_{pw} must be known. A, A_∞, a_w are obtained from three separate experiments: 1) FTIR-MIR *in situ* measurement of asphalt/model siliceous aggregate specimens exposed to water, 2) FTIR-MIR analysis of water in contact with the asphalt-free substrates, and 3) water uptake in asphalt films, respectively. In this study, A, the FTIR-MIR absorbance corresponding to the total amount of water detected at a given exposure time, was taken directly from the experiment. Value of A_∞, the FTIR-MIR maximum absorbance of liquid water, for the asphalt-free substrate was taken from Reference 25. Values of d_{pa} and d_{pw} , the penetration depths in asphalt and water, respectively, were calculated from Equation 2 using 45-degree incident angle, and the refractive indices of the substrate, asphalt, and water.

1.3. Experimental Procedure

This section briefly describes the experimental procedure used to measure the thickness of the water layer at the interface between an asphalt and a model siliceous substrate by the FTIR-MIR technique. Complete details on the materials used, specimen preparations, and experimental setup are given in Reference 24. The asphalts were from five Strategic Highway Research Program (SHRP) straight core asphalts: AAC-1, AAD-1, AAG-1, AAK-1, and AAM-1. Their selective properties are summarized in Table 1.

Table 1. Some properties of five core SHRP straight asphalts selected for the study (27)

SHRP Asphalt	Asphaltene (heptane) content, %	compat. index	Element, Mass Fraction % N	O	S	Viscosity kPa.s, 25 °C
AAC-1	9.8	2.40	0.7	0.9	1.9	94.540
AAD-1	20.2	1.44	0.8	0.9	6.9	40.570
AAG-1	5.0	3.97	1.1	1.1	1.3	354.000
AAK-1	20.1	1.22	0.7	0.8	6.4	107.700
AAM-1	3.7	5.93	0.6	0.5	1.2	112,300

The asphalts were selected based on their wide range of difference in dispersibility (or compatibility), asphaltene contents, and heteroatomic nonhydrocarbon constituents (e.g., N and S). The model siliceous substrates were 50 mm x 10 mm x 3 mm spectroscopic grade, 45° parallelogram silicon (Si) internal reflection elements (IRE). The as-received Si IREs had a 2.07-nm thick layer of native oxide (SiO_2, refractive index = 1.46) on their surfaces, as measured by ellipsometry. At ambient conditions (22 °C and 45 % relative humidity), the surfaces of this substrate should be covered with silanol (SiOH) groups and adsorbed water, similar to the functional groups on a silica surface (28). The surfaces of the Si substrate used were presumably to have the chemical structure illustrated in Figure 2. The hydrated, SiO_2-covered, 50 mm x 10 mm x 3 mm, 45°, parallelogram Si substrate used in the study is designated as the model siliceous aggregate.

Specimens were prepared by applying hot asphalt (at 60 °C) to one surface of the substrate using the draw down technique. Masking tape strips placed along the substrate were used to control the asphalt film thickness. A water chamber, which has an inlet and an outlet to introduce and remove water, was attached to each asphalt-coated specimen. The specimen with the water chamber attached was positioned vertically in an accessory holder. The specimen configuration and experimental setup for measuring in situ water at the asphalt/aggregate interface is shown in Figure 3. With this configuration, the only pathway for water migration from the environment to the interface is through the thickness of the asphalt film within the walls of the chamber. Further, since the infrared radiation entered and propagated within the substrate, there was no interference of liquid water from the environmental chamber or water vapor in the spectrometer compartment. Note that with the thickness of the substrate and the configuration used, there were 17 reflections generated within the substrate before exiting. The use of a thinner substrate, a longer substrate, a smaller angle of incidence, or a combination of these factors would increase the detectability of water at the asphalt/substrate interface by the FTIR-MIR technique.
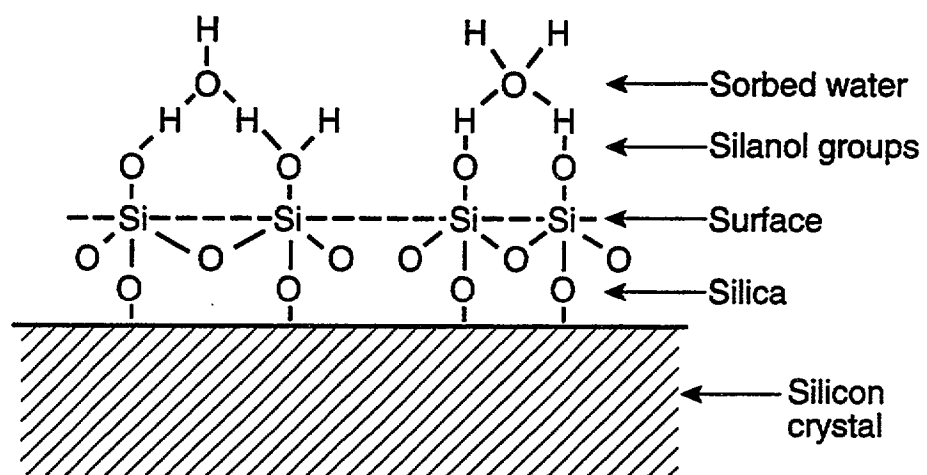
Figure 2. *Postulated surface chemical structure of the model siliceous aggregate.*
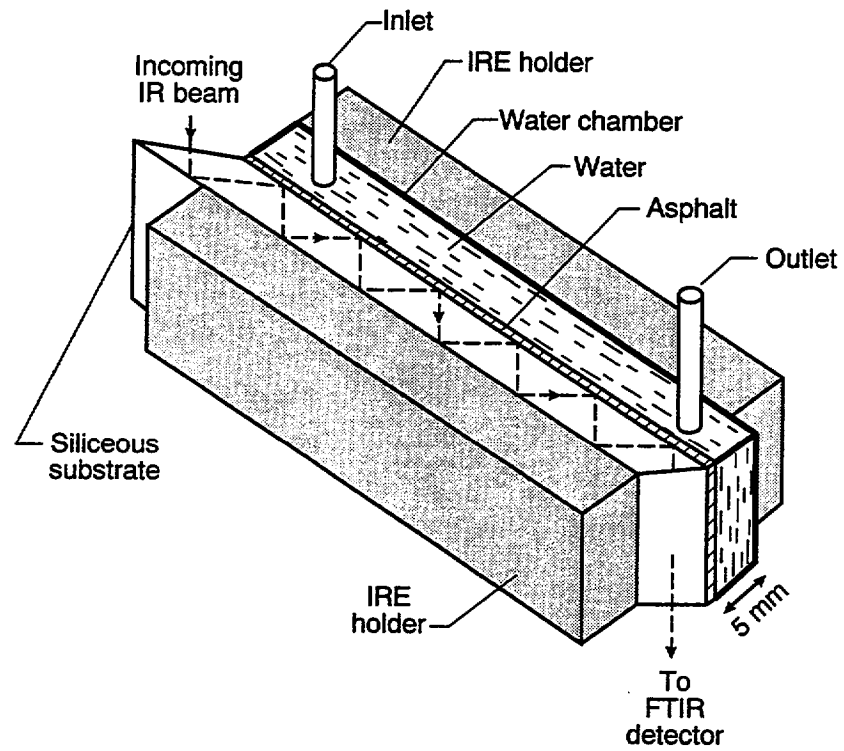
Figure 3. *Specimen configuration and experimental setup for in situ measurement of water at the asphalt/model siliceous aggregate interface.*

After adding water to the chamber and placing the specimen assembly in the spectrometer, FTIR-MIR spectra were taken automatically every 15 minutes without disturbance to the instrument until the experiment was complete. All spectra were the result of 32 co-additions and were collected at a 4 cm^{-1} resolution throughout the 1200 cm^{-1} - 4000 cm^{-1} range. Unpolarized light at an incident angle of 45° was used. All spectra were plotted in the absorbance (A) mode. Difference spectra were obtained by subtracting the spectrum of specimen before exposure from the spectrum of the same specimen but after exposing to water at a particular time interval. Quantitative analyses were performed using the peak height method, which measures the absorbance at the maximum of the bands of interest. It should be noted that, except for one case where two specimens were used, results on the quantity of the water layer at the asphalt/substrate measured by the analytical FTIR-MIR technique were determined from only one specimen; therefore, there are no uncertainty values accompanying these data.

Since this was an *in situ* measurement, no errors due to the accessory adjustment, specimen changing, spectrometer and environmental chamber conditions, and optical realignments were introduced in obtaining the spectra. Thus, any changes in the spectra were a direct result of the effect of water entering the asphalt/aggregate specimen. Further, because the asphalt was applied directly to the MIR element, errors resulting from variations in the contact between them were avoided. Until now, lack of control of the contact between the sample and the element has hindered the broad application of the FTIR-MIR technique for quantitative studies.

1.4. Results

1.4.1. FTIR-MIR Analysis of Water in the Asphalt/Siliceous Substrate Interfacial Region

In order to monitor changes resulting from water entering the interface between an asphalt and a model siliceous substrate, it was necessary to examine the FTIR-MIR spectral characteristics of water and of the asphalt/siliceous substrate system before water exposure. Figure 4a presents a typical FTIR-MIR spectrum in the 1200 cm^{-1} to 4000 cm^{-1} region of a straight asphalt (AAD in this case) applied to the model siliceous substrate before exposure to water . (FTIR-MIR spectra of the other four asphalts are given in Reference 24.) Because Si absorbs infrared radiation strongly in the region below 1200 cm^{-1}, bands below this frequency were deemed not reliable for analysis and therefore were not included. The thickness of this asphalt film was 60 μm $\pm$ 13 μm. Typical straight asphalts show four main bands associated with the CH groups in the 2800 cm^{-1} to 3000 cm^{-1} and 1350 cm^{-1} to 1500 cm^{-1} regions. Figure 4a shows little evidence of IR absorption due to the polar OH/NH groups, which generally occur in the in the 3100 cm^{-1} to 3700 cm^{1} region. This is probably due to the combination of low concentration of these groups in the asphalts and the shallow probing depth of the MIR technique in this frequency region. On the other hand, the FTIR-MIR spectrum of liquid water on the same substrate (Figure 4b) shows a broad strong band in the 3000 cm^{-1} to 3650 cm^{-1} region, due to the OH stretching, and at 1640 cm^{-}^{1}, due to HOH bending, of molecular water. The shoulder (around 3250 cm^{1}) on the right side of the water OH stretching band is due to the contribution of the overtone of the bending mode. It is noted that the probing depths of the evanescent wave in asphalt and water at the OH stretching

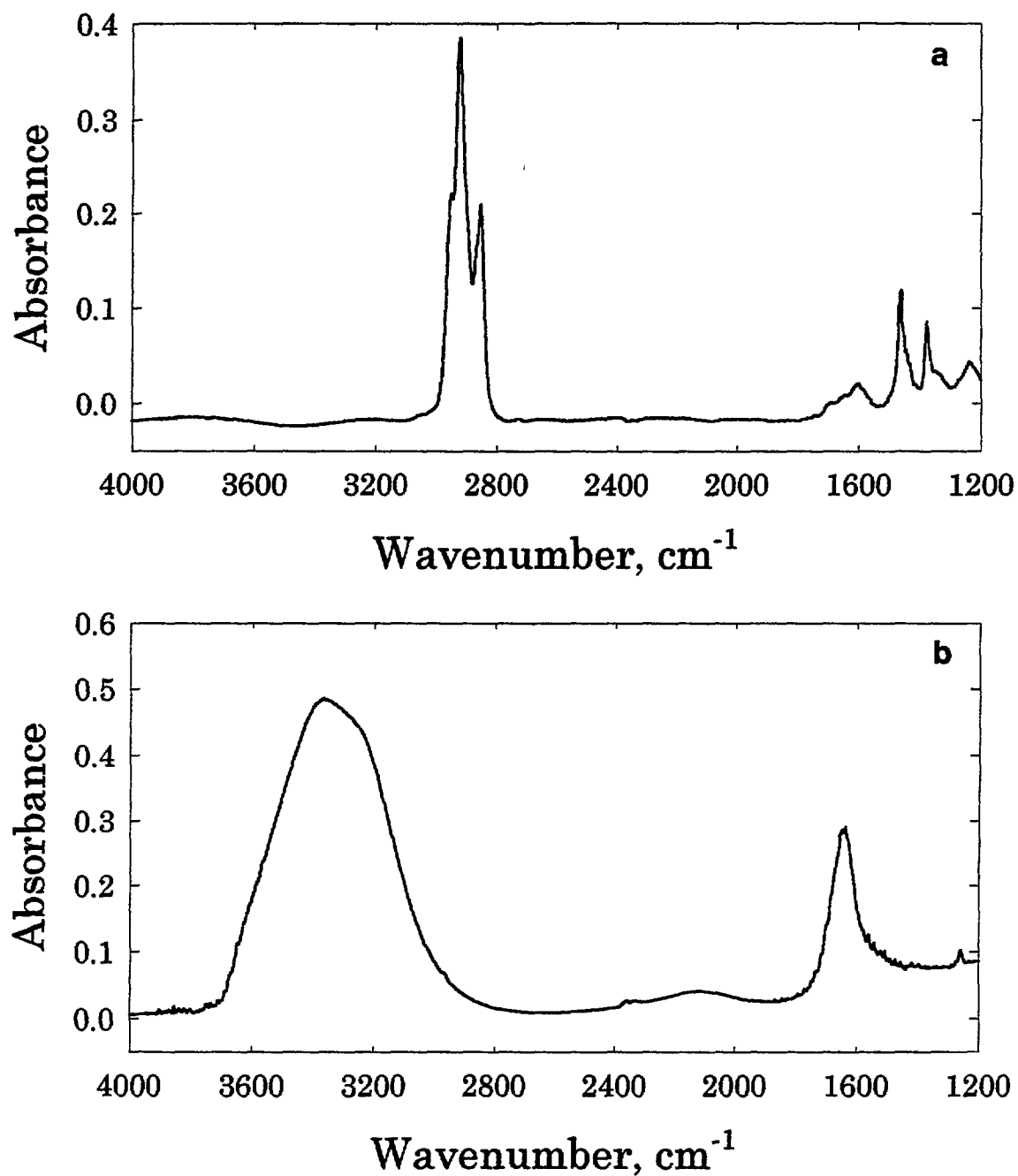band for a Si substrate are <0.75 μm.

Figure 4. a) Typical FTIR-MIR spectrum of a straight asphalt on the model siliceous substrate before exposure to water, and b) FTIR-MIR spectrum of liquid water on the model siliceous substrate.

11

Figure 5 illustrates one example of a series of typical unprocessed FTIR-MIR spectra for an asphalt applied to the model siliceous aggregate before and after exposure to water for different times. The thickness of the asphalt film of this specimen was 63 μm$\pm$10 μm. These spectra were obtained by ratioing the spectra of the exposed specimen against the corresponding spectrum of the background (the spectrum of the environment in the spectrometer).

Although the effect of water is evident in the 3000 cm^{-1} to 3650 cm^{-1} and 1625 cm^{-1} to 1645 cm^{-1} regions, these spectra still include information of the asphalt material. To provide data for quantitative analysis of water at the interface, difference spectra were acquired by subtracting the spectrum collected before exposure from those obtained at different water exposure times.

One example of the difference spectra in the 1500 cm^{-1} to 4000 cm^{-1} region of an asphalt (AAC in this case) on the model substrate after exposure to distilled water for different times is displayed in Figure 6. If water has not entered the asphalt/substrate interfacial region, all difference spectra would be straight lines, with the exception of the intensity fluctuations of the CO_2 bands from the air in the spectrometer. Bands above or below the baseline of a difference spectrum indicate an increase or a decrease, respectively, of the concentration of a chemical functional group as a result of water exposure.

Figure 6 clearly shows that the intensity of the water band in the 3000 cm^{-1}-3650 cm^{-1} region increased, while the intensity of the asphalt bands, e.g., at 2922 cm^{-1}, decreased with time of exposure to water. The intensity decreases of the coating bands, together with the intensity of the water bands as a function of exposure time, may be explained only by the water entering the asphalt/substrate interface. This is because the probing depths of the evanescent wave in water-saturated and water-free asphalts are essentially the same. As the thickness of the water at the interface increased, the amount of the asphalt material within the probing depth decreased because the asphalt film was pushed further away from the substrate surface. The intensity, expressed as peak height, of the water band at 3400 cm^{-1} is suitable for quantitative analysis of water at the asphalt/model siliceous aggregate interface. The water bending mode was found not suitable for the analysis because it does not appear for low water concentrations (29).

Figure 7 presents plots of intensity (peak height of the absorption band) changes of the water OH stretching band as a function of exposure time for the five asphalts. Although, there are some minor fluctuations of some data points, the trends of water accumulated in the interfacial region are evident. In general, except for AAD which did not appear to take up any more water after 50 h, all other specimens continue to pickup water for more than 100 h. Water initially entered the interfacial region at a high rate, but then slowed down. The rates at which water entered the interfacial region were quite different for the five asphalts. The rates of decrease of the bands associated with the asphalt (e.g., band at 2922 cm^{-1}) also followed the same trend with the water bands (24).

12
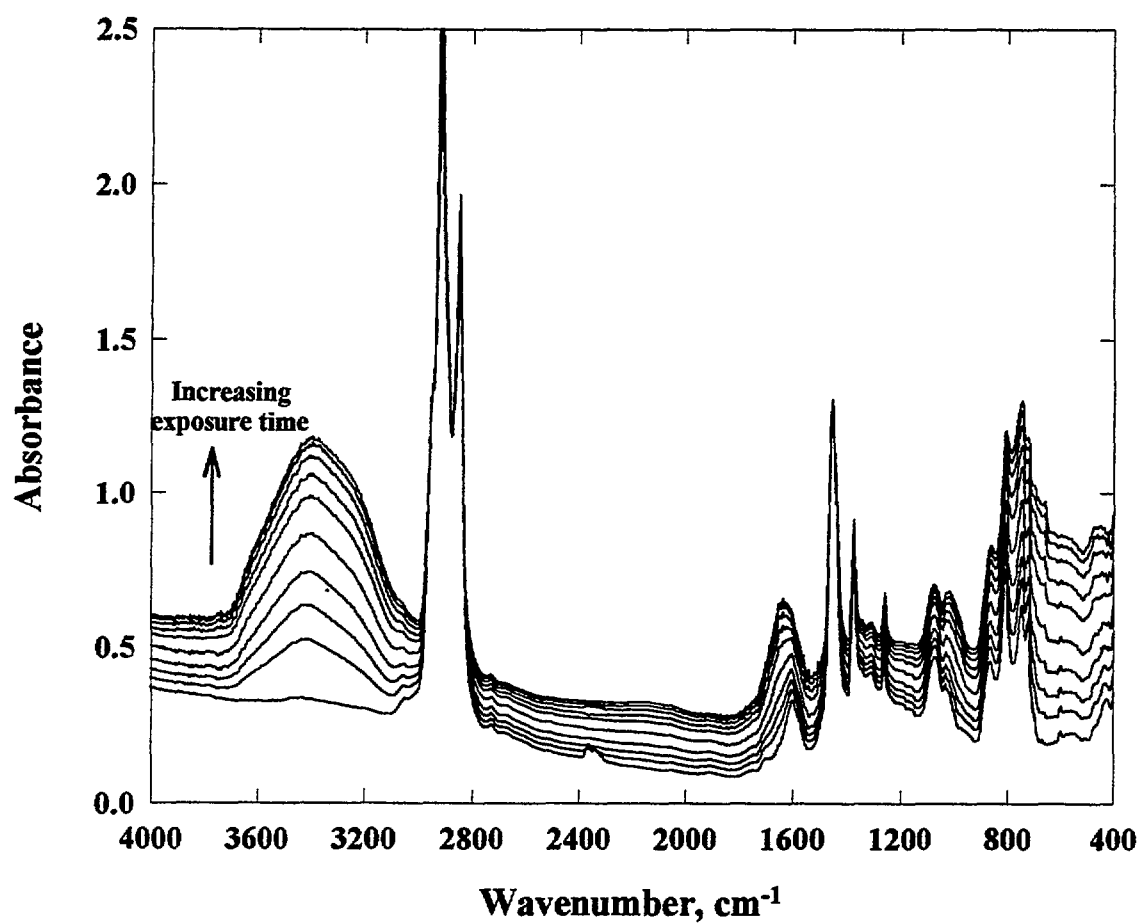
Figure 5. *Typical FTIR-MIR spectra of an asphalt/model siliceous aggregate specimen after exposure to water.*
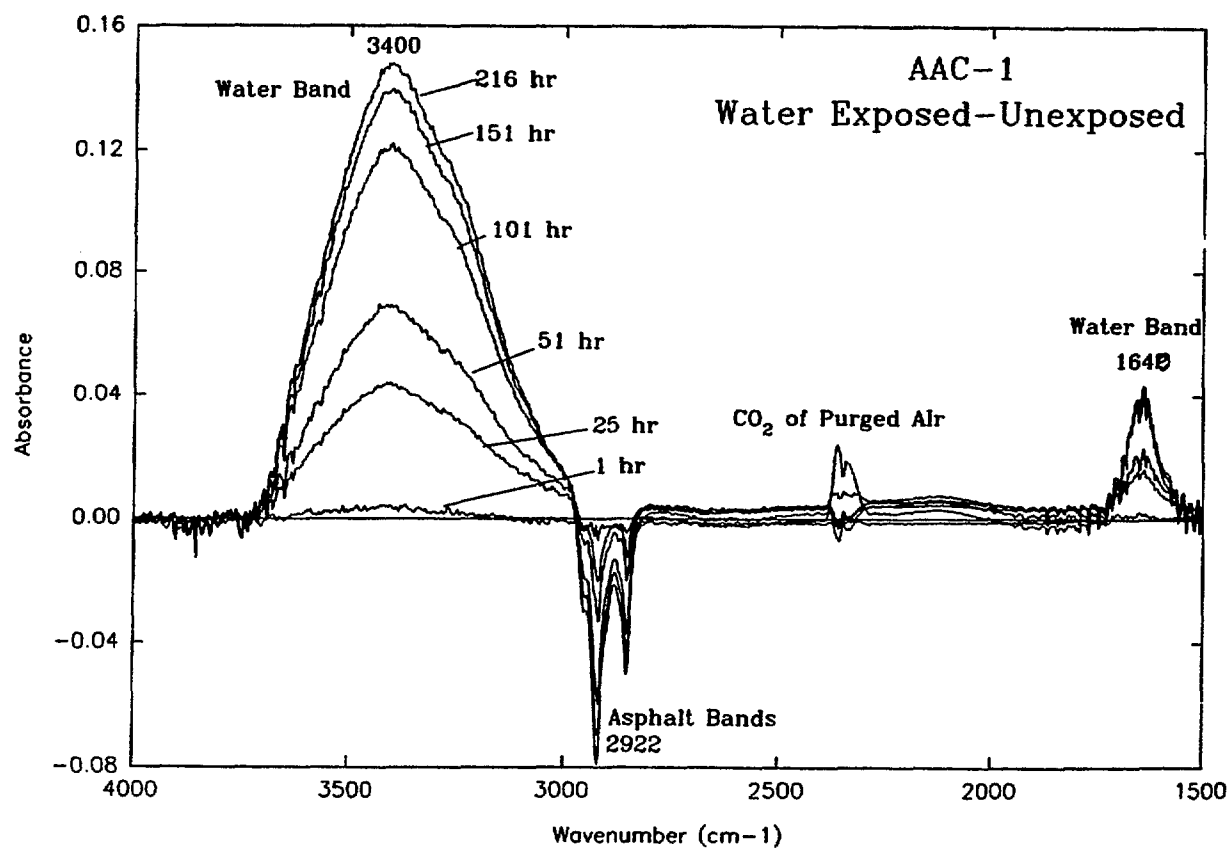
Figure 6. *An example of FTIR-MIR difference spectra (water exposed - unexposed) of an asphalt/model siliceous aggregate specimen exposed to water for different times.*
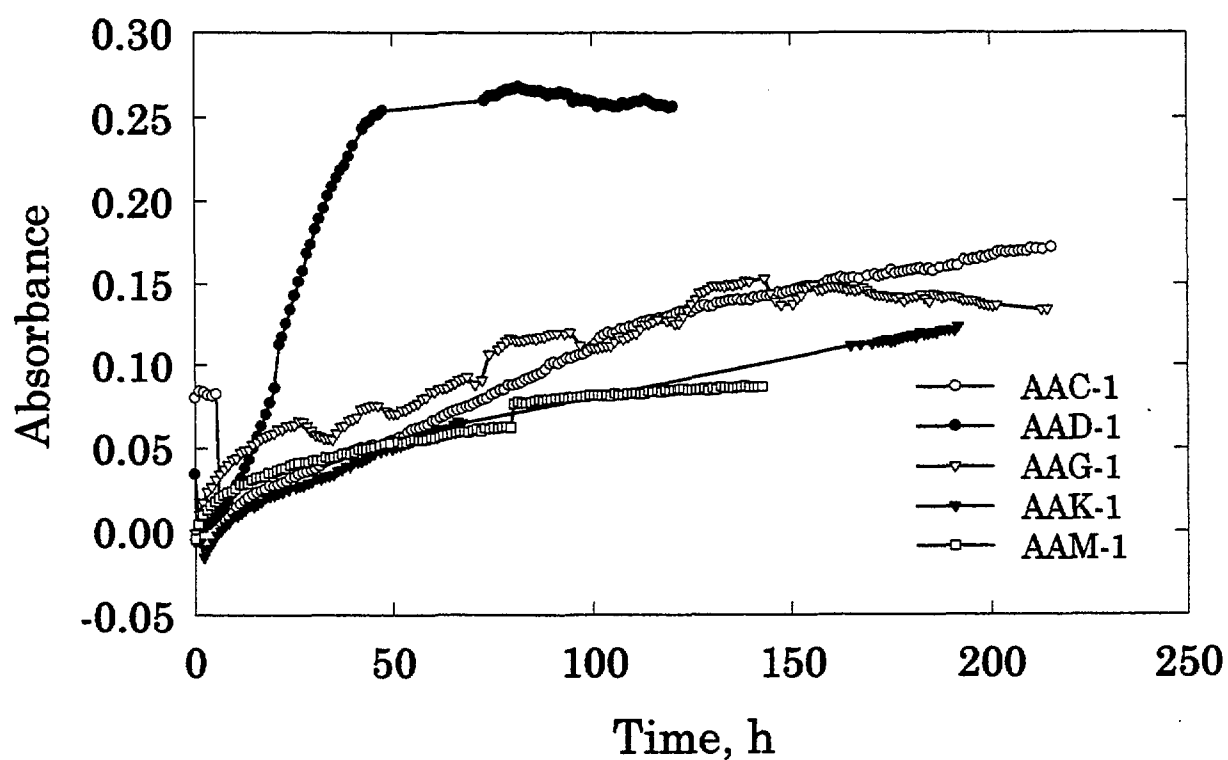
Figure 7. *Intensity increase of water OH group as a function of exposure time for five SHRP asphalts on a model siliceous aggregate. (Each dot represents one data point.)*

1.4.2. Quantification of Water at the Asphalt/Model Siliceous Substrate Interface

1.4.2.1. Model Verification

The FTIR-MIR intensity displayed in Figure 7 corresponds to the total amount of water detected. This quantity comprised water at the asphalt/substrate interface and water in the asphalt film within the evanescent wave probing depth, as depicted in Figure 1 and mathematically expressed in Equation 1. Subtracting the water uptake within the evanescent wave depth in the asphalt from the total water detected yields the values on water at the asphalt/substrate interface.

Before using Equation 3 for quantifying water at the interface between an asphalt and a siliceous aggregate, the main question that must be addressed is how good are the assumptions and model used for deriving this equation? One way to answer this question is to subject an organic-coated substrate that has a water-resistance interface to a water environment. From the well-known mechanism of adhesion bonding and durability of epoxy/E-glass fiber composites, such an interface may exist. Consequently, specimens made of a two-part epoxy applied to a silane-treated SiO_2-Si substrate were prepared. Details on the chemical structure of the epoxy, silane coupling agent, procedure for silane treatment on substrate surface are given elsewhere (30). The substrate and the procedure used for collecting the spectra are similar to those described in Section 1.3 of this study.

The results (average of two specimens) on the amount and thickness of the water layer at the epoxy film/silane-treated substrate interface calculated using Equations 3 and 5 are presented in Figure 8. The parameters used for the calculation are given in Reference (25). Figure 8 clearly indicates that, essentially, no or little water had entered the interface of this specimen.

The interfacial water layer result obtained by FTIR-MIR (Figure 8) is in good agreement with the adhesion data of the same epoxy resin applied to a similar substrate, which showed that epoxy/silane-treated SiO_2-Si substrate system lost little of its bonding strength even after a prolonged exposure to water at 24 °C (31). The result is also consistent with the chemical bonding theory used for explaining the hydrolytic stability of polymer composites made with silane-treated E glass fiber (32). If no water accumulated at the interface, then the total water detected is due to solely water sorbed in the epoxy resin layer near the interface. This is predicted by Equation 1 and observed experimentally in Figure 8. For such a case, only the second term of Equation 1 exists. Apparently, the epoxy-coated, silane-treated siliceous substrate has a hydrolytically-stable interface and the water was incapable of replacing the strong chemical bonds between the silane coupling agent and the siliceous substrate or between the silane agent and the epoxy resin. The result of Figure 8 provides the first evidence that the model developed and presented here is valid for quantifying water at the asphalt/siliceous interface.
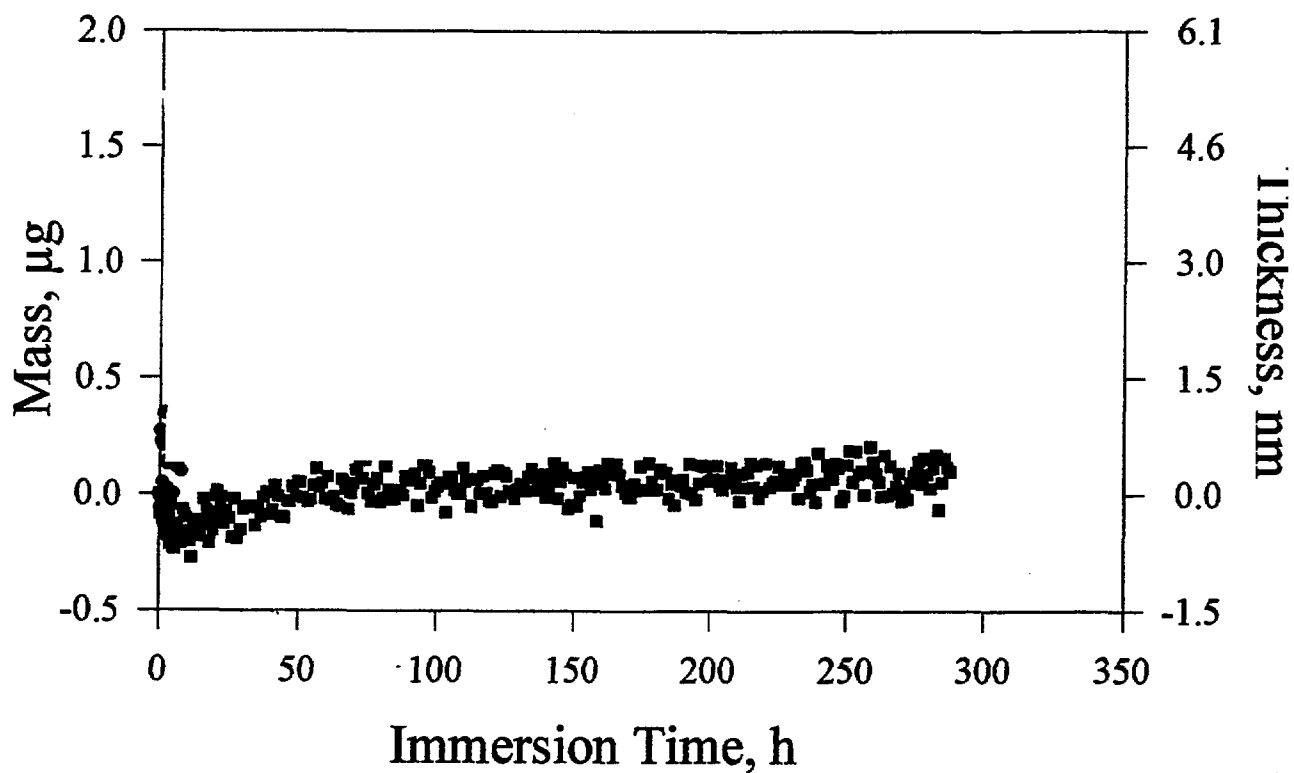
16

Figure 8. *Amount and thickness of the water layer at the interface between a model epoxy and a silane-treated siliceous substrate as a function of water exposure, showing essentially no water entered the interface of this specimen. (Each dot represents one data point.)*

1.4.2.2. Thickness and Amount of Water at the Asphalt/Model Siliceous Substrate Interface

In order to obtain the thickness l and amount Q_i of water at the asphalt/substrate interface using Equations 3 and 5, A, A_∞, a_w, d_{pc} and d_{pw} must be known. A, the total IR absorbance of water in the specimen at each exposure time is taken directly from Figure 7. A_∞, the maximum IR absorbance of water is given in Figure 4b. a_w, water fraction of water in the film is interpolated from the asphalt water uptake results given in Reference 24. The uptake experiments were conducted using the gravimetric method for asphalts coated on aluminum sheets. Only the amount of water within the penetration depth of the evanescent wave is used for the calculation. Discussion on the assumptions and errors resulting from the interpolation has been presented in detail elsewhere (29).

Values of d_{pa} and d_{pw}, the penetration depths in asphalt and water, respectively, were taken from Figure 9, which shows the penetration depth of the evanescent wave as a function of infrared wavelength. The curves on this figure were calculated using Equation 2, a 45° incident angle, and the refractive indices of 3.42 for Si substrate, 1.55 for asphalt, and 1.32 for water. The refractive index of asphalt was calculated from the data taken in Reference 33. As can be seen in Figure 9, the FTIR-MIR technique can probe rather deeply in the asphalt, particularly at long wavelengths. The results also showed that d_p in asphalt is slightly greater than in water and this difference increases with increasing wavelength. At the wavelength of interest, 2.94 μm (the OH stretching of water, 3400 cm^{-1}), d_{pa} and d_{pw} values in asphalt and water are 0.243 μm and 0.225 μm, respectively. At this wavelength, there is only a small difference (0.018 μm) in the d_p value whether asphalt or water is in the interfacial region. Due to exponential decay, it has been shown experimentally that 87% of the signal obtained by the MIR technique is from the d_p depth (17). Based on this result, the water signals observed in Figure 5 must be from water close to the asphalt/substrate interface.

Results on the thickness and amount of the water layer at the asphalt/model siliceous substrate interface as a function of exposure time for five SHRP asphalts are given in Figure 10. The mass of the interfacial water layer can also obtained by using Equation 5, a water density (ρ) of 1 Mg/m^3, and a surface area (a) of 329 mm^2. In general, the amounts of water within the penetration depths of the five asphalts are very small, <5 %, as compared to the total water detected (24). These results are consistent with other studies, which show that, for organic films such as asphalt, water detected is mainly from the water layer at the film/substrate interface (25,30,34).
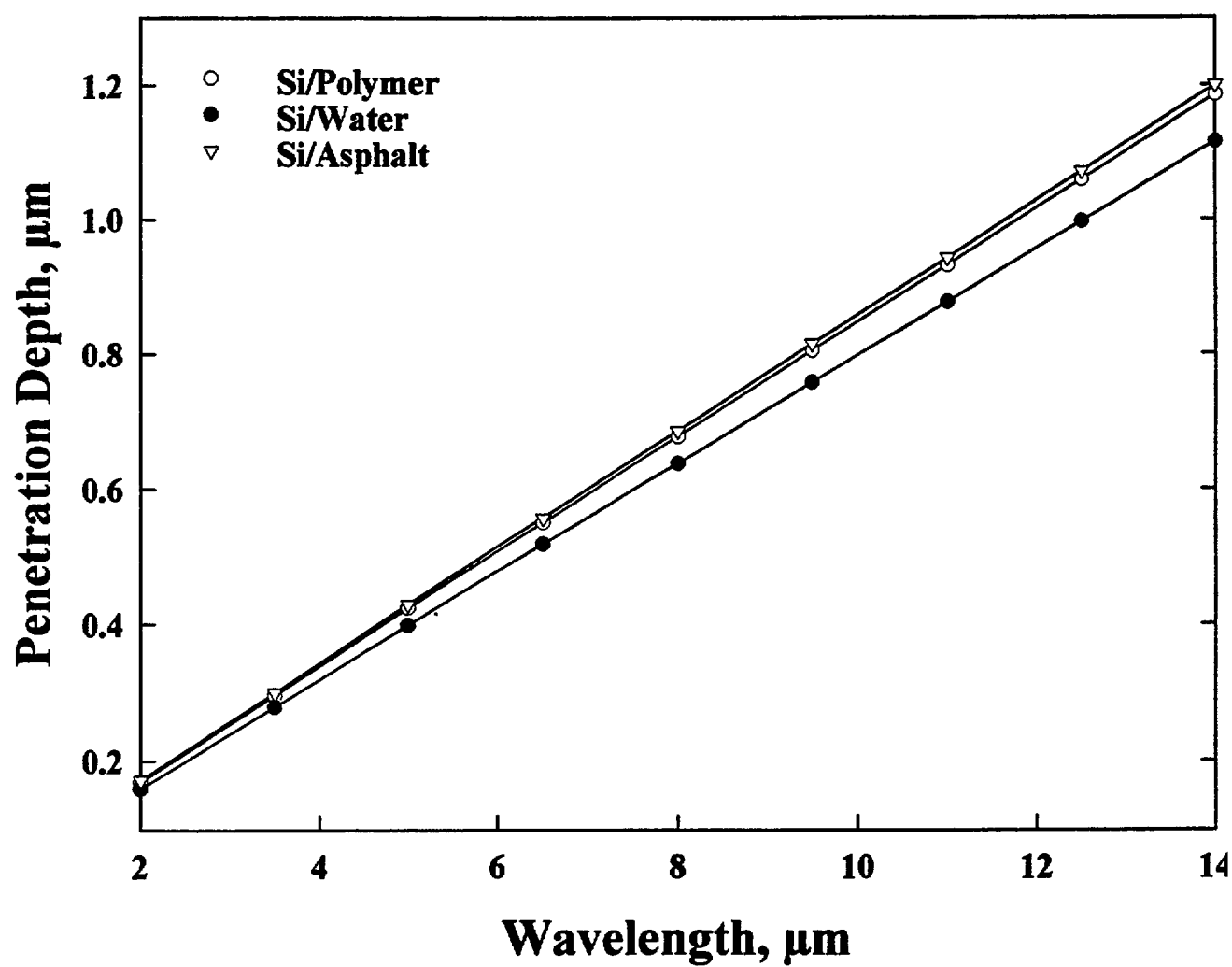
Figure 9. *Penetration depth of the evanescent wave in asphalt and in water as a function of wavelength.*

Figure 10 shows that thickness of the water layer at the asphalt/model siliceous substrate interface was different for the five asphalts. The thickness of the water layer for the AAD/substrate interface increased rapidly and remained constant after approximately 45 h of immersion, but the water layer thickness for the AAC specimen increased slowly at first and did not level off even after 100 h of exposure. Water layers at the interface of AAG, AAK and AAM asphalts also increased less rapidly than that of the AAD specimen and seemed to slow down after 75 h. For prolonged immersion, e.g. 90 h, the water layer at the asphalt/model siliceous substrate interface was thickest for AAD (90 nm) and thinnest for AAM (25 nm). The thickness values for AAC, AAG and AAK specimens were 35 nm, 45 nm, and 35 nm, respectively, at the same exposure time. The results suggest that the AAD/siliceous system was less resistant to water stripping than the AAM specimen. It is noted that since this method detects water after it has migrated through the asphalt film thickness, it is suitable for measuring the diffusion coefficients of water in a film applied to a substrate, as demonstrated for asphalt (24) and other organic films (34).
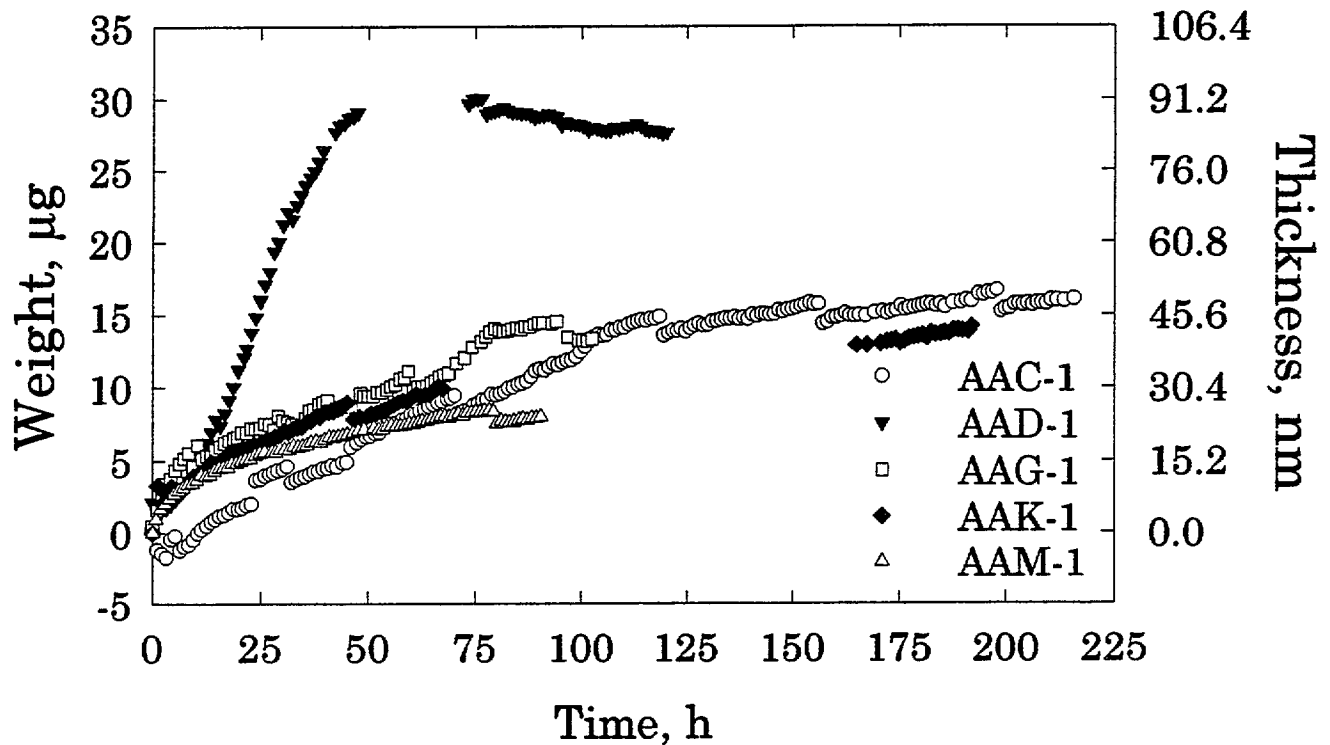
Figure 10.   *Amount and thickness of the water layer at the asphalt/model siliceous aggregate interface for five SHRP asphalts. (Each dot represents a data point.)*

2. MEASUREMENT OF ADHESION LOSS OF ASPHALT/AGGREGATE SYSTEM EXPOSED TO WATER

2.1. Experimental Section

2.1.1. Materials and Specimen Preparation

This experiment measures the bonding strength of asphalts applied to flat substrates exposed to water as a function of time. Five SHRP asphalts, AAC-1, AAD-1, AAG-1, AAK-1 and AAM-1 applied to two aggregates, granite and soda-lime glass plates, were used for this study. Both granite and soda-lime glass plates have dimensions of 304 mm x 304 mm sides and 6 mm thickness. The granite plates were obtained from a local store and the mate-finish side was used for the test. Although the exact type and source of the granite substrate were unknown, common granite stones contain, on the average, the following major components 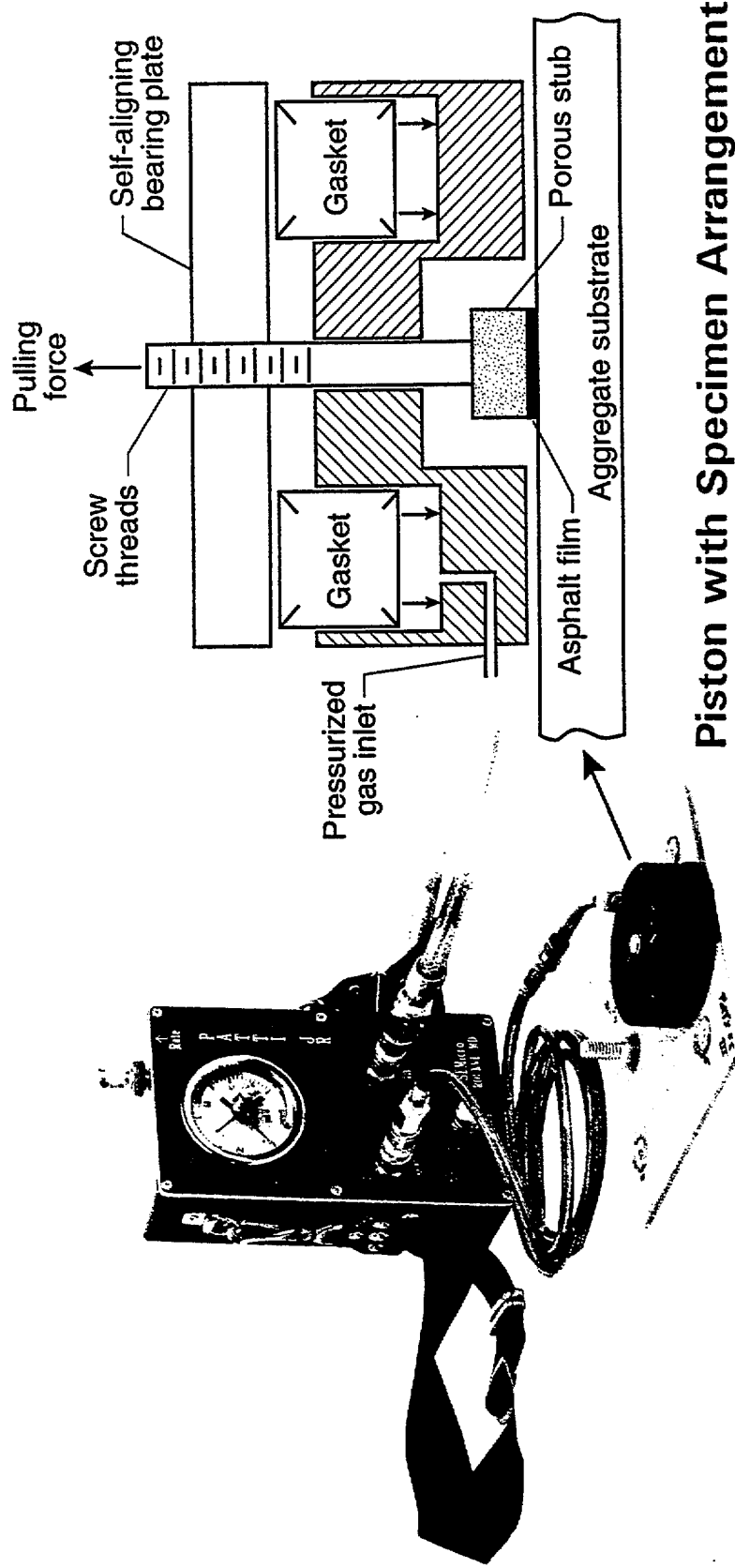(mass fraction): 72 % SiO_2, 13.6 % Al_2O_3, 8.5 % Na_2O and K_2O, and <2 % MgO and CaO (35). Soda-lime glass typically contains 72 % SiO_2, 13% Na_2O and K_2O, 13 % CaO and MgO, and 1 % Al_2O_3 (36).

Granite and glass plates were washed thoroughly with a detergent and rinsed repeatedly with distilled water followed by methanol and dried with hot air before use. Methanol was used to remove water on the substrate surface. The asphalts were heated to 70 °C and applied to an approximately 12 mm diameter, confined area of the substrates, which were also heated to 70 °C. A preliminary study employed two pieces of copper wire, having desired diameter and a length of about 6 mm, placed parallel to each other on each asphalt-coated area to control the asphalt film thickness. However, our later study showed that mixing a small fraction (0.5 % based on asphalt mass) of glass beads having the desired diameter in the hot asphalt is a more convenient method for controlling the asphalt thickness. The glass bead procedure, which has been used in the aircraft industry to produce uniform adhesive thickness, substantially reduced the time to prepare asphalt specimens for adhesion loss evaluations. The thicknesses were verified by measurement using a thickness gage.

After applying asphalt to the substrate, a flat, porous stub with a screw attached to it was pressed onto each asphalt-coated area (see Figure 11). The porous stubs, having a diameter of 12 mm and a thickness of 6 mm, were cut from bricks used for construction. One advantage of the porous stub is to provide cavities and increased surface area for enhancing the adhesive bonding of asphalt to the stub. However, the uniqueness of the porous stub is to allow water to migrate through the asphalt film thickness to the interface. Had the stubs been made of nonporous materials, such as that used in the pull-off adhesion test for organic film on a substrate (37), water would migrate to the asphalt/substrate interface from the edges and not through the asphalt film thickness. This would take a long exposure time for water to cover the entire interface. Such surface transport from the edges would cause a gradual adhesion loss, starting from the edge of the specimen and moving toward the center of the specimen as exposure continues. This adhesion loss pattern is due to the loss of the bonding area rather than due to the buildup of the water layer at the asphalt/substrate interface, and thus is not desirable for this study.

21

Self-aligning
bearing plate

Gasket

Porous stub

Pulling
force

Gasket

Screw
threads

Asphalt film

Aggregate substrate

Pressurized
gas inlet

Piston with Specimen Arrangement

Pneumatic Adhesion Tester

Figure 11. *Components of apparatus and specimen arrangement used for testing adhesion loss of asphalt/flat substrate specimens exposed to water.*

Each stub-attached, 12 mm asphalt-coated area is one specimen. A total of 18 stub-attached specimens were prepared on each substrate plate. Excess asphalt around each specimen was removed by a razor blade. Specimens were then conditioned for three days at ambient environment (22 °C and 45 % relative humidity). Specimens were immersed in distilled water at room temperature (22 °C), withdrawn from the water container at each time interval (8 time intervals), and immediately tested for bond strength while the specimens were still wet.

It should be mentioned that several preliminary studies were conducted to provide base line parameters used for the adhesion loss measurement of asphalts applied to the substrates. The first experiment was to optimize the thickness of the asphalt film. The results showed that, although a thickness range between 100 μm and 300 μm was found suitable for the adhesion test, an asphalt thickness of around 200 μm was found most convenient to prepare the specimens. Thinner asphalt films required more laborious efforts to align the loading feature perpendicular to the substrate surface. On the other hand, it was difficult to obtain an uniform thickness for films >300 μm because asphalt flows quite easily at 70 °C. Further, thick asphalt films required long immersion times in water before testing. The second experiment was an investigation of a well-characterized, porous brass material commonly used in water filtering as a substitute for the brick stub. It was found that water did not flow well through this material, perhaps due to the presence of a release agent used during the manufacturing. Soaking these stubs in a hot nonpolar solvent followed by a hot polar solvent resulted in satisfactory water flow in these stubs. However, because the procedure to clean these stubs was laborious and involved volatile materials, the use of a porous brass material for testing the bonding strength of asphalt/flat aggregate system in the presence of water was abandoned. Another study was to determine the effect of trapped air during the specimen preparation on the adhesion; the result showed that there was no significant difference on the bonding strength (dry) of specimens prepared in air and in a vacuum.

2.1.2. Adhesion Measurement Instrumentation

Figure 11 depicts a schematic of the instrument used to measure the bonding strengths of an asphalt applied to a flat aggregate exposed to water. The main features of this device are a portable pneumatic adhesion tester, a piston, and a loading fixture consisting of a porous stub attached to a screw. The pneumatic adhesion tester, which was developed and patented at NIST, is now commercially available for less than 3000 US dollars. This instrument is now part of the ASTM D4541"Pull-Off Strength of Coatings using Portable Adhesion Testers" (37). Among the portable testers included in the ASTM D4541 standard, the pneumatic adhesion tester gives the lowest coefficients of variance of results within and between the laboratories.

The procedure for preparing and testing the adhesion of an asphalt on a flat aggregate before and after exposure to water is described below. After conditioning or exposing a specimen to water, the piston is placed over the stub-attached loading fixture and against the substrate surface. Compressed air is introduced, and as air pressure in the piston increases, an air tight seal is formed between the piston gasket and the substrate. When the pressure in the piston exceeds the cohesive strength of the asphalt or the adhesion between the asphalt and the substrate, the

specimen breaks, either cohesively in the asphalt or at the asphalt/substrate interface. Pressure at break was recorded and converted into stress, using a calibration curve. All results of the bonding strength at each exposure time were the average of six specimens. The coefficient of variation (COV) and standard deviation were determined.

2.2. Results

Figures 12 and 13 show the results of the bonding strengths of five SHRP asphalts on the soda glass and granite substrates, respectively, as a function of exposure to distilled water. All five asphalts lost adhesion rapidly as a function of exposure time. However, the rates of decrease and times-to-failure were different for the five asphalts and for two substrates. All asphalts on the soda glass failed at much earlier times than those on the granite substrate. On granite (Figure 13), the bonding strengths of AAK-1, AAC-1 and AAD-1, which did not appear to differ between one from another, lost most of their bonding strengths within 20 h of exposure. AAG-1 failed after 50 h while AAM-1 did not fail until after 180 h. On glass, AAD-1 lost most of its adhesion within 4 h, and the other four, behaved similarly, after 8 h or 16 h of exposure in water. On both glass and granite substrates, the failure modes changed during water exposure. In the dry state, all failures occurred in the asphalts (cohesive failure). But the locus of failure appeared to change (by the naked eye) to a mixed mode, i.e. cohesive and adhesive (breaking at the asphalt/substrate interface), or purely adhesive as exposure continued.

The results showed that the coefficient of variance (COV) of the bonding strength (between specimens) of all specimens before exposure was less than seven percent. This indicates that the pneumatic pull-off adhesion test is a good method for evaluating the bonding strength of an asphalt on a flat aggregate. The COV seemed to be higher when testing wet specimens, particularly when the mode of failure changed from cohesive to adhesive or to a mixed mode. The higher COV of bonding strength after exposure to water was probably due to the inhomogeneous nature of the asphaltic materials, which contain various polar and water-soluble species. This hypothesis was substantiated by light microscopy analysis of specimens after the test, which revealed that the fractured surfaces consisted of small gray areas of asphalt, where the asphalt was probably emulsified, and larger black areas of "unmodified" asphalt.

Based on the results of this study, time-to-failure at a given residual bonding strength in water may be used as a criterion for comparing the relative stripping resistance of asphalts on flat aggregates. Although further study and analysis are needed to establish the level of residual adhesion appropriate for stripping determination, the results presented demonstrated that the use of a pneumatic pull-off adhesion tester combined with a porous stub is suitable for measuring the bonding strength of an asphalt on an aggregate in the dry condition as well as in the presence of water. This test provides useful data on the relative stripping resistance of different asphalts on a substrate. The method is quantitative, quick, simple, reproducible, insensitive to operator, and portable; it can be used in the laboratory and in the field. The pneumatic adhesion tester is commercially available and relatively inexpensive (<$3000) and the porous stubs can be easily made.

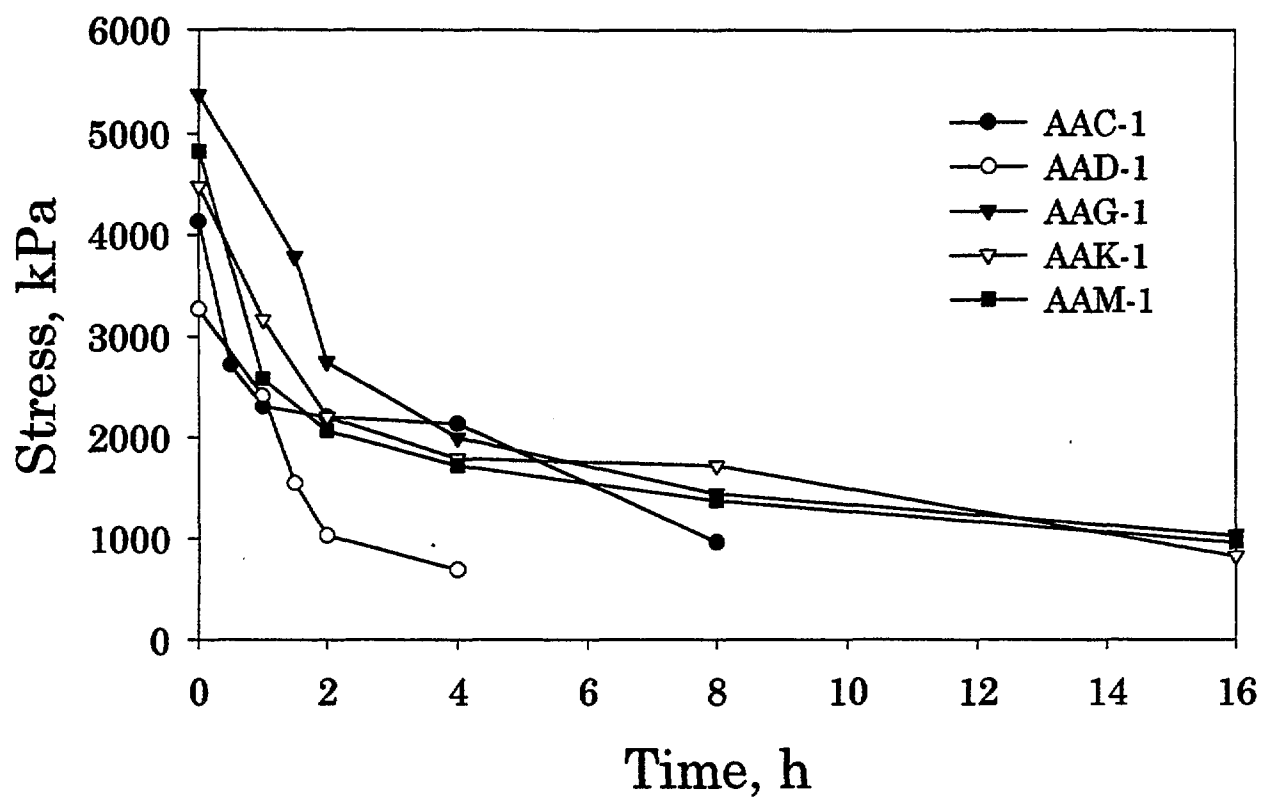*Figure 12.* *Bonding strengths of five SHRP asphalts on a soda-lime glass substrate as a function of exposure to water.*
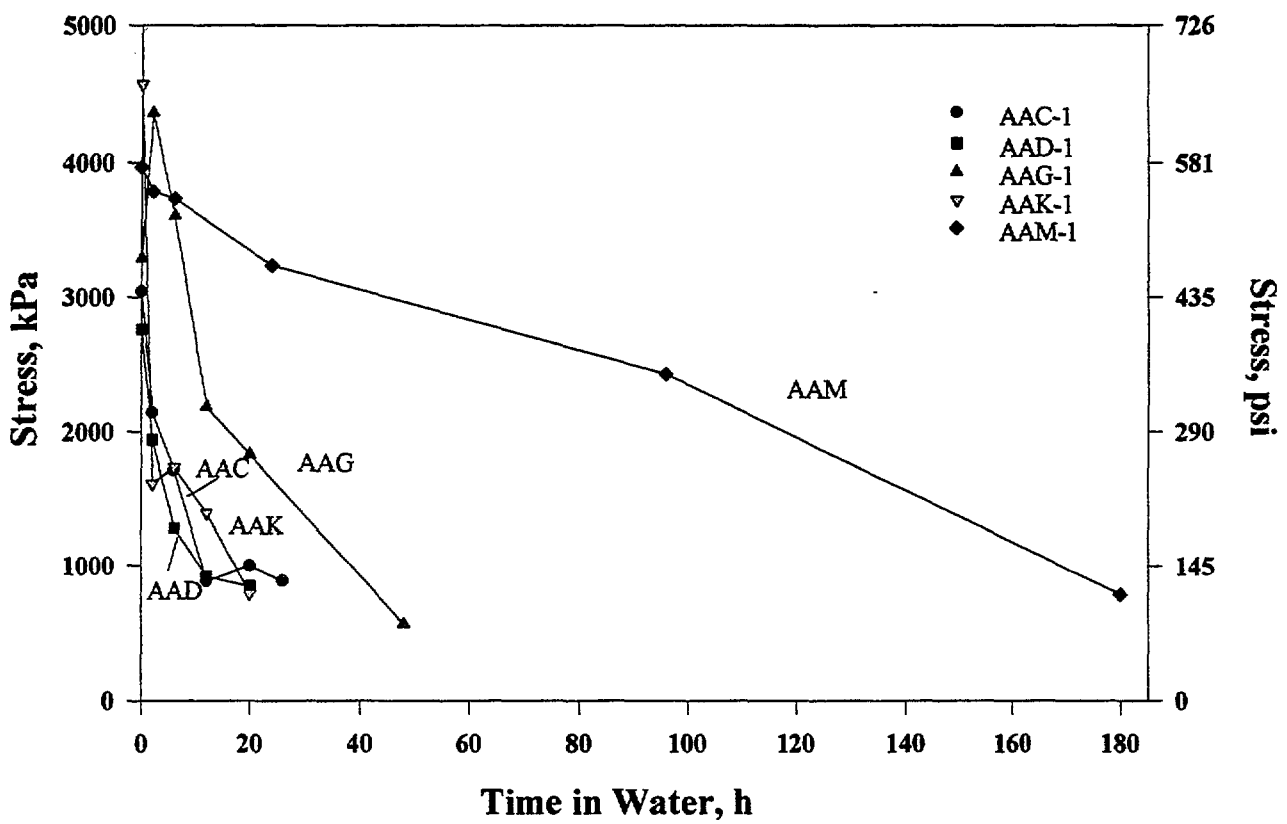
Figure 13. *Bonding strengths of five SHRP asphalts on a granite substrate as a function of exposure to water.*

26

2.3. Discussion

The more rapid and greater adhesion loss of asphalts on the soda-lime glass than those of asphalts on the granite substrate requires some discussion, because it may help to explain the difference in stripping characteristics of asphalts on dissimilar aggregates. The difference in the adhesion loss behavior of the same asphalts on the two substrates may be explained by the chemical composition difference between the two substrates.

As presented in the experimental section, both granite and soda-lime glass substrates compose approximately the same amounts of SiO_2. However, soda-lime glass contains substantially higher contents of the alkaline oxides (MgO and CaO) and alkaline earth oxides (K_2O and Na_2O) and a lower content of Al_2O_3. The nonsilica components in the amorphous glass are known to exist as microheterogeneities estimated to be from 15 Å to 200 Å (38). These oxides are hygroscopic so that water adsorption on glass is characterized by the hydration of these oxide microheterogeneities. Thus, soda-lime glasses have been found the most hygroscopic, but even a more water-resistant E-glass powder adsorbs twice as much water as the silica (39). The rapid and multiple layer adsorption of water on soda glass surface has been attributed to the hydration of hygroscopic inclusions in the glass (40). Further, it has been verified that the adsorption of tens of molecular layers of water on polar solids at partial pressures just below saturation is due to the presence of hygroscopic contaminants (41). Even at a relative humidity of 50 %, a surface contaminated with 10^{-7} g/cm² of potassium hydroxide would adsorb the equivalent of five molecular layers of water.

Not only does soda glass adsorbs thick water films but this water has been found strongly alkaline. For example, it has been demonstrated years ago that the visible water film formed from subsaturation vapor pressure on the inside of a freshly blown glass tube could be titrated with an acid solution (42). Similarly, the thin water layer between two soda glass plates has been known to test alkaline with a pH indicator. The alkalinity is probably due to the conversion of alkaline earth oxides (Na_2O and K_2O) to hydroxides in the presence of water. From this analysis, it is expected that not only the buildup of the water layer at the interface for asphalt/soda glass is faster and thicker but also the water layer is more alkaline than that for the asphalt/granite samples. The stronger alkalinity would accelerate the hydrolysis of the asphalt/glass bonds, while the faster water accumulation at the interface would decrease more rapidly the adhesion of the systems. Further, the presence of a larger amount of hygroscopic materials at the interface for the soda glass substrate also creates a greater osmotic difference between the outside and the interface for this system than that for the granite. The greater osmotic pressure would result in a higher rate of water transport from the outside to the interface for the soda glass than the granite specimens.

Another factor that may contribute for smaller adhesion loss of the asphalt/granite than that for the asphalt/soda glass sample is the higher concentration of Al_2O_3 in the granite substrate. The effect of Al_2O_3 may be explained by its strong interaction with asphalt. The interaction between a solid and a liquid can be estimated from measurement of the heat of immersion, which also directly relates to the zero point of charge (pH of the aqueous solution at which the oxide is

uncharged). The heat of immersion of Al_2O_3 in water (7.3×10^{-2} J/m^2) is almost four times of that of SiO_2 in water (1.8×10^{-2} J/m^2) (43). Obviously, the interaction is stronger when the oxide bond (M-O) is highly ionic, such as Al_2O_3, and weaker when the M-O is covalent, such as in SiO. Although similar information for asphalt is not available, its interactions with the oxides should follow the same trend as those of the water because both water and asphalt are weakly acidic. Thus, asphalt, being an acidic material, is expected to form strong bonds with basic aggregates, such as aluminum oxides or limestone, and weak bonds with acidic aggregates, such as silica. This is consistent with the acid-base interaction theory (44).

All four factors cited above; that is, the strong alkalinity, the faster and thicker interfacial water film buildup, the higher osmotic pressure, and the fewer number of strong Al_2O_3/asphalt bonds probably account for most of the greater adhesion loss of an asphalt on a soda glass substrate than that of an asphalt on a granite aggregate. The same analogy may be used as an explanation for the differences in the adhesion loss or stripping susceptibility of asphalt on different substrates. The SHRP study on asphalt-aggregate interactions has demonstrated that aggregate chemistry is a much more important factor than the asphalt composition for both adhesion and sensitivity to water of asphalt/aggregate mixtures (45).

3. RELATION BETWEEN ADHESION LOSS AND THICKNESS OF THE WATER LAYER AT THE ASPHALT/SILICEOUS AGGREGATE INTERFACE

3.1. Introduction

The buildup of water of many monolayers thick at the coating/substrate interface has been postulated as the main cause of adhesion loss when an organic-coated substrate is exposed to water or high relative humidities (46). However, there has been no study to correlate the water layer at the organic film/substrate interface with the adhesion loss. The main reason for this is the lack of quantitative information on both the interfacial water layer and the adhesion loss of organic film/substrate systems exposed to aqueous environments. Sections 1 and 2 provided quantitative data on the water layer at the asphalt/substrate interface and the adhesion loss as a function of exposure to water. This section will examine the relationship between these two quantities for both asphalt and other organic film/siliceous aggregate systems.

3.2. Relation between Interfacial Water and Adhesion Loss for Asphalt/Siliceous Aggregate Systems

The following discussion involves the relationship between interfacial water and adhesion loss for asphalt/siliceous aggregate systems. The discussion is based on the water layer at the asphalt/model substrate given in Figure 10 and the adhesion loss data presented in Figures 12 and 13 for five SHRP asphalts on both glass and granite substrates.

As shown in Figure 10, after 50 h of exposure the thickness of the water layer at the interface for the AAD asphalt specimen was substantially greater than that of the other four asphalts, which did not differ among themselves. Except for a difference in times of exposure, these results show a good agreement with either the time-of-failure at 1500 kPa or residual bonding strength after 2 h exposure for the adhesion loss of asphalts on soda glass (Figure 12). For the asphalt/granite system (Figure 13), there is a general agreement between the adhesion loss and interfacial water layer obtained at long exposure times. For example, at 90-h exposure the thicknesses of the interfacial water layer for AAD and AAM asphalt specimens were 90 nm and 25 nm, respectively; the thicknesses of AAC, AAG and AAK specimens were in the same range for the same exposure time. These results are in agreement with the time-to-failure at 1500 pKa of the adhesion loss data of the same asphalts on a granite substrate given in Figure 13. Although further analysis is needed, the results show that the thicker water layer at the asphalt/siliceous interface generally corresponds to the shorter the time-of-failure of the system.

Both the interfacial water and adhesion loss data obtained in this study are consistent with moisture sensitivity tests results of core SHRP asphalts on siliceous aggregates given in SHRP-A003B report (45). For example, the numbers of repeated free-thaw cycles (moisture sensitivity test) for AAM, AAC, AAK, AAG, and AAD on the RA granite (>a mass fraction of 96 % granite) were given to be 50, 36, 10, 7 and 5, respectively (the longer the number of repeated cycles the more

29

stripping resistance of a asphalt/aggregate mixture to water). This is in general agreement with thicknesses of the interfacial water layer at 90-h exposure (Figure 10) for the same order and asphalts on the model siliceous aggregate.

3.3. Relation between Interfacial Water and Adhesion Loss of Polymer/Model Siliceous System

Although there is a general agreement between the interfacial water layer given in Figure 10 and adhesion loss presented in Figures 12 and 13 for asphalt/siliceous aggregate specimens, it is not expected to find a strong correlation between these two sets of data. The main reason for this is due to the difference in the substrates used for the two experiments, i.e., a model siliceous substrate was used for the water at the interface measurement and soda glass and granite substrates were used for the adhesion loss study. As discussed in Section 2.3, the chemistry of the aggregate surface plays a key role in the adhesion loss of asphalt on an aggregate in water. For that reason, an experiment was carried out where the substrates and organic films used for measurements of interfacial water layer were the same as those used for measuring the adhesion loss. This experiment used specimens of a solvent-free epoxy coating on untreated and silane-treated SiO_2-Si substrates. The epoxy was a stoichiometric mixture of a low molecular weight diglycidyl ether of bisphenol A resin and a polyethertramine curing agent. There was no solvent in the epoxy coating. Since it was a stoichiometric mixture of low molecular weight materials, it was expected that only a little amount of amine was left after the curing. The interfacial water measurement was carried out using 50 mm x 10 mm x 3 mm SiO_2-covered Si internal reflection element (IRE), similar to those used for interfacial water measurement for asphalt as described in Section 1. For the adhesion loss measurement, specimens of the same epoxy coatings applied to Si wafers having a diameter of 4 mm were used. The surfaces of the Si wafers had a native SiO_2 layer of about 2.5 nm thick and, under ambient conditions, they should be covered with hydroxyl groups, similar to that of the Si IRE. Thus, in this experiment the substrates used for both interfacial water and adhesion loss measurements were similar. Both prisms and wafers were used with and without a silane surface treatment. The substrates were cleaned with acetone followed by methanol, and dried with hot air before use. Silane treated substrates were prepared by immersing cleaned Si prisms and wafers for 30 minutes in an acidified (pH=4) water solution containing a mass fraction of 0.1% aminoethylaminopropyltrimethoxysilane. The silane treated substrates were dried for 10 minutes at 110 °C before applying the epoxy coatings. The coatings were applied on Si IRE and wafers using the drawdown technique.

The procedure used for determining the amount of water at the epoxy film/model siliceous substrate interface was the same as described in Section 1 for asphalts. Duplicate specimens were used for each film/substrate system. The measurements of adhesion loss of epoxy coatings on Si wafers as a function of exposure in water were conducted using a wet peel adhesion tester described in Reference 47. The results were the average of 12 specimens, which derived from two wafers.
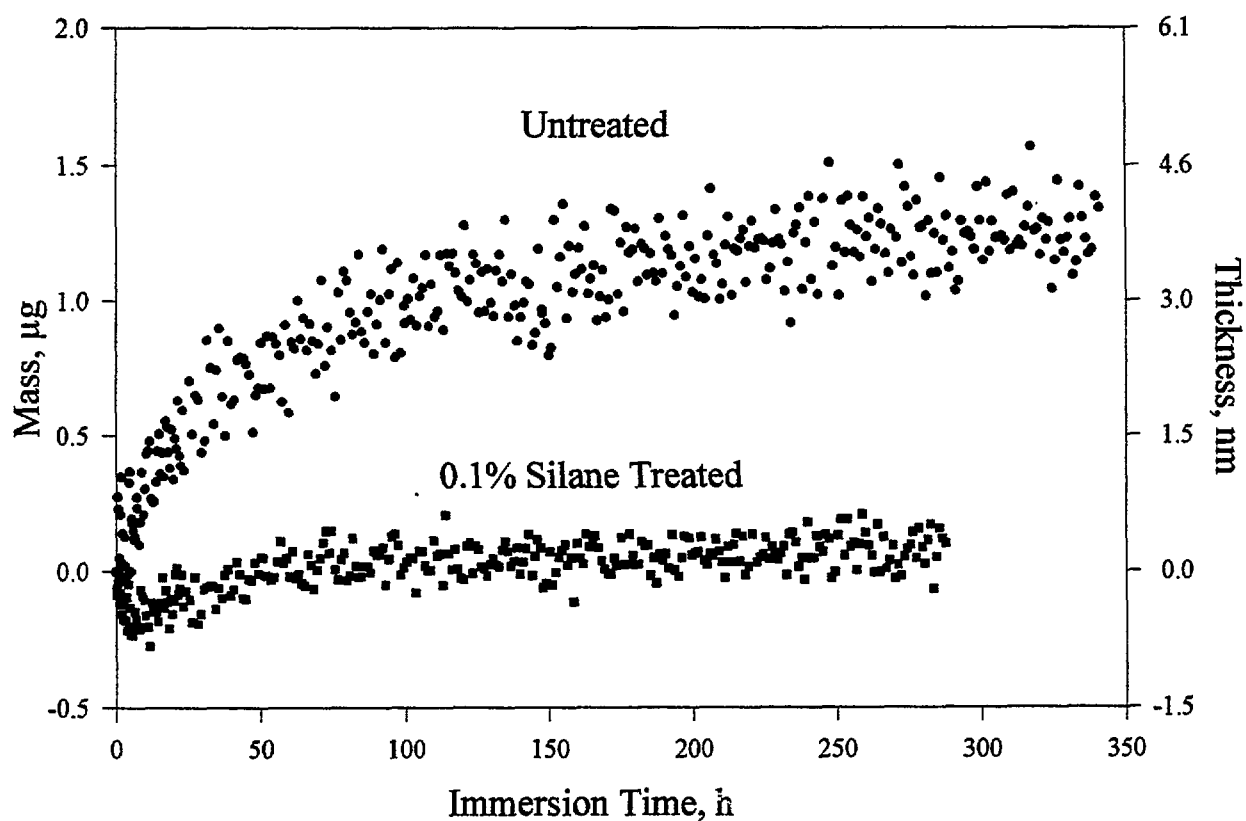
Figure 14. *Amount and thickness of the water layer at the interface as a function of water exposure for: a) epoxy/untreated model siliceous substrate system, and b) epoxy/silane-treated model siliceous substrate system.*

Figure 14 presents the results on the amount and thickness of the water layer at the film/substrate interface as function of exposure time obtained by FTIR-MIR technique for epoxy coating on untreated and silane-treated Si IRE. Essentially, no water entered the interface of the epoxy/silane-treated substrate specimens, but some water (about 10 monolayers) had built up at the interface of the untreated substrates. Figure 15 gives the results on the adhesion loss as a function of time exposed to distilled water for the same epoxy film on Si wafers. Silane treatment greatly reduced the adhesion loss of the solvent-free epoxy specimens. Similar relationship between interfacial water and shear strength has also been found for epoxy/E-glass fiber composites (31).

Although more data and analysis are needed to determine precisely the range of the amount of water at the interface that causes the loss in adhesion, the results of this experiment indicate that there is a good correlation between the thickness of the water layer at the organic film/siliceous substrate interface and the adhesion loss of the same system exposed to water. That is, the more water entering the organic film/siliceous substrate interface the greater the adhesion loss of the same film/substrate system. These results support the above conclusion on the general agreement between the interfacial water layer and adhesion loss for asphalt specimens. The correlation between data obtained by the two techniques developed in this work indicates that information on the water layer at interface may be used for assessing the stripping resistance of an asphalt/siliceous mixture. Thus, instead of carrying out elaborate water debonding or water sensitive tests, which often require multiple replicates to provide any meaningful results, FTIR-MIR technique may be used for determining the stripping resistance of asphalts on a siliceous aggregate. This technique may also be used for conveniently studying the effects of many variables affecting the stripping of asphalts on a siliceous substrate such as asphalt type, antistripping agents and their concentrations, environmental temperature, substrate surface contaminants, salted water, and rained water. The application of FTIR-MIR technique for evaluating the performance of antistripping agents is presented in the following section.
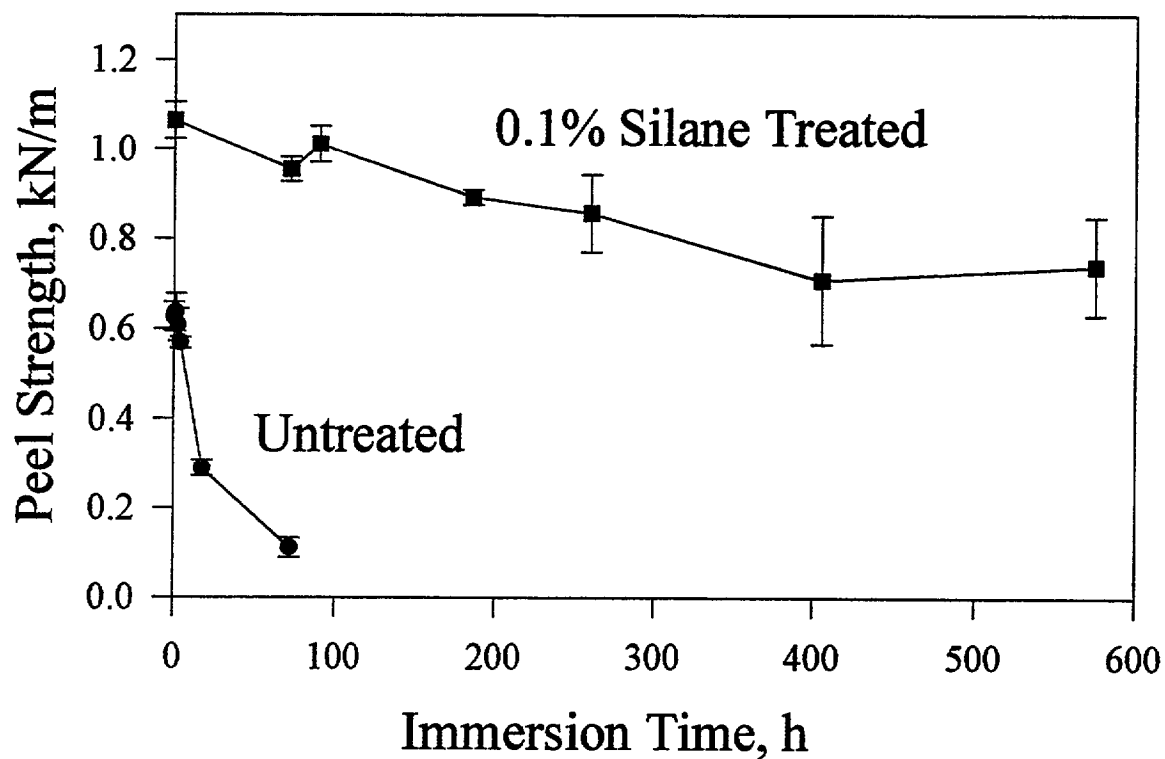
Figure 15. Bonding strengths as a function of water exposure for specimens of an epoxy coating on untreated and silane-treated model substrates.

3.4. Evaluation of Effectiveness of Antistripping Agents by FTIR-MIR Technique

Based on the results presented above, FTIR-MIR was used to evaluate the relative performance of four antistripping agents, using the same model substrate (SiO_2-covered Si) and experimental setup shown in Figure 3. The antistripping agents (supplied by SHRP program) were MAS-021-001 (hydrated lime), MAS-016-001 (a polyphosphate based), MAS-022-001 (a low grade aliphatic polyamine), and MAS-023-001 (a high grade polyamine). The specimens were prepared by mixing thoroughly 1 % (based on asphalt mass) of antistrippping agents in a hot asphalt (AAD) at 60 °C. Each hot anistripping-containing asphalt mixture was then applied to the model siliceous substrate. The thickness of asphalt film used in this experiment was approximately 200 µm ± 15 µm, as determined by a thickness gage. FTIR-MIR spectra were taken automatically every 15 minutes until the experiment was complete.

Figure 16 presents FTIR intensity (absorbance) of the band for water at the asphalt/siliceous interface as a function of time exposure to distilled water for an asphalt containing a mass fraction of 1 % of four different antistripping agents. As indicated earlier, the intensity is directly proportional to the amount or thickness of the water layer at interface. The results showed that there was little water at the interface of the asphalt containing MAS-021-001 (hydrated lime) antistripping agent, but substantial water had entered the interface for asphalt specimen containing MAS-022-001 (low grade aliphatic polyamine) after 250 hours of exposure. Values of water at the interface for the polyphosphate (MAS-016-001) and high grade polyamine (MAS-023-001) containing asphalts were in the between. These results suggest that hydrated lime appeared to be the most effective and low grade aliphatic amine was the least effective among the four agents studied.
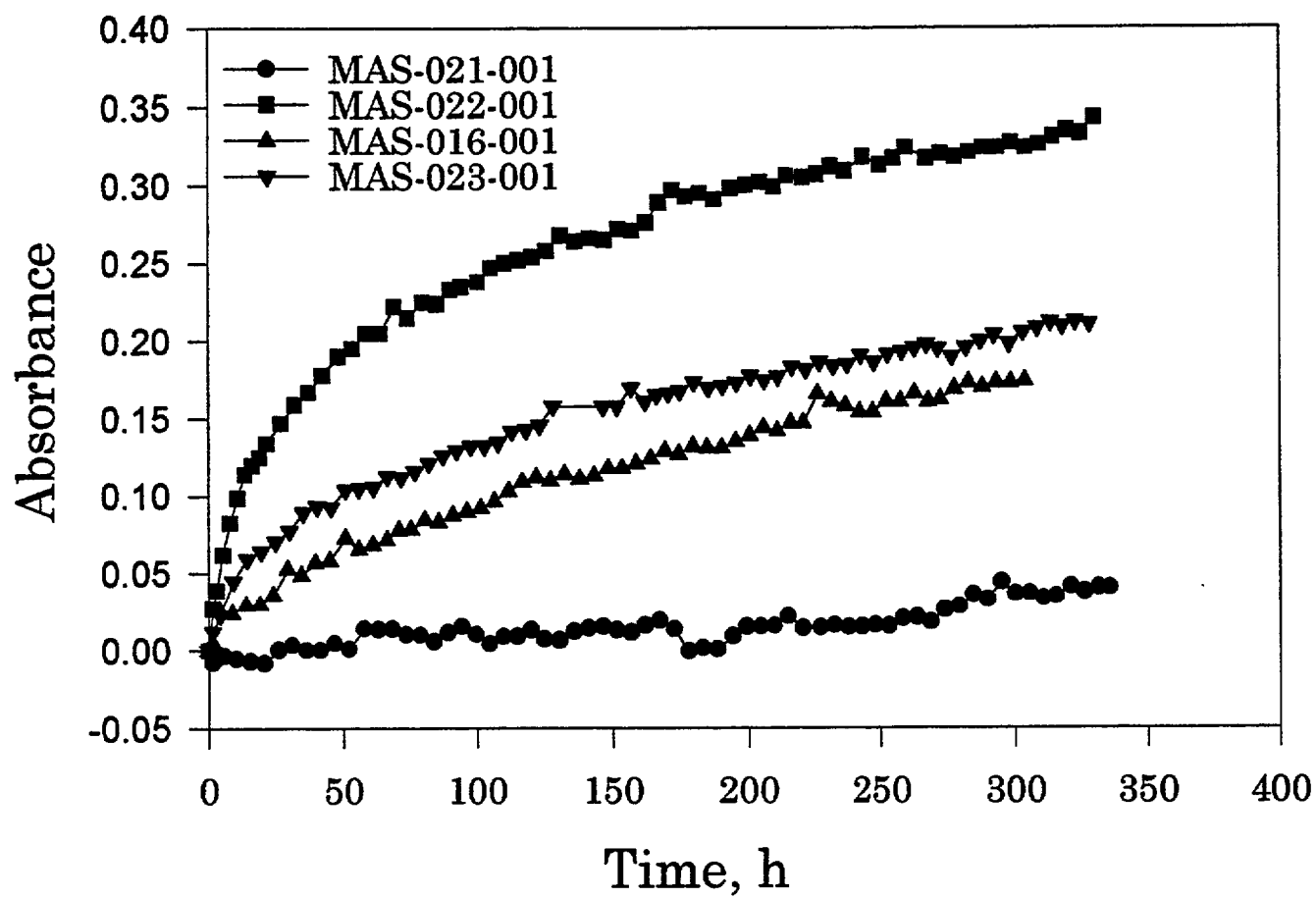
Figure 16. *FTIR-MIR intensity of the water layer at the asphalt/siliceous substrate interface for different antistripping agents.*

4. MECHANISM OF WATER STRIPPING OF ASPHALT ON A SILICEOUS AGGREGATE

The results of Figure 10 show that at long exposure times many monolayers of water had accumulated at the asphalt/siliceous aggregate interface (one water monolayer is approximately 0.3 nm). Indeed, this was the case because we observed substantial amounts of liquid water beneath the asphalt films as they were peeled from the model siliceous substrate at the conclusion of the experiment. These results are consistent with extensive data on organic coatings and water sorption measurements at silica surfaces. Leidheiser and Funke (46), in an intensive review of water disbondment of organic coated metals, had given examples and cited references to support the evidence of the presence of multilayers of water at the organic coating/metal interface. Another evidence is from water adsorption studies on high-energy surfaces. For example, Zettlemoyer and coworkers (48,49) noted that monolayer of water on ferric and nickel oxides occurs at low relative humidities, but multilayers exist at a relative humidity of 90%. Bowden and Throssell (50) found that up to 20 molecular layers of water were on aluminum, iron, and SiO_2 surfaces at ambient temperatures and humidities. Similarly, Debye and van Beek (51) reported that silica powder, washed with water and then dried at 100 °C, retained a water adsorbed layer tens of nanometers thick. The presence of multilayers of sorbed water on the surface of different types of glass has been discussed briefly by Bascom (52).

The adsorbed water layers closest to the surface are strongly bonded and difficult to remove. Therefore, the presence of a monolayer of water at the asphalt/aggregate interface would probably not interfere with the adhesion of an asphalt/aggregate mixture. However, increasing the coverage of water will, at some point, affect the strength of the asphalt/aggregate bonds. This is substantiated by the adhesion loss data given in Figures 12 and 13 for asphalts and in Figure 15 for an epoxy coating on a siliceous substrate. Further backing for the adhesion loss of organic-coated substrates in water comes from extensive results on the durability of adhesive bondings (53) and organic coatings on metals (46,54,55) These studies demonstrated that the bonding strength of an organic film/untreated, high energy substrate system decreases significantly after exposure to water and high humidities. Further, the decrease is accelerated with increasing temperature.

The stripping susceptibility of an asphalt from siliceous aggregate may be best understood from the interaction energy standpoint. The bonding between asphalt, an organic material, and a siliceous aggregate is governed mostly by weak secondary forces, which are generally less than 25 kJ/mole (4). On the other hand, the magnitude of the bonds which water form with oxide surfaces are substantially higher, typically in the 40-65 kJ/mole (7). Consequently, the affinity of water for a siliceous aggregate is greater than that of asphalt to the same aggregate. Further, free surface energy analysis has also shown that the reversible work of adhesion between an organic film and an oxide, including SiO_2, is highly negative in the presence of water (4), implying that the asphalt/siliceous substrate bonds are not stable in water. This means that water is likely to enter the interface and displace the asphalt from a siliceous aggregate when an asphalt/siliceous mixture is exposed to water or to high relative humidities. This postulation is consistent with the acid-base (an electrostatic interaction) theory proposed by Fowkes (44), who used this theory to

explain for the water susceptibility of asphalt/granite systems and water resistance of asphalt/limestone mixtures. The asphalt, with its low basicity and high acidity, interacts weakly with the acidic SiO_2 but adheres strongly with basic aggregates, such as limestone. The strong asphalt/basic aggregate bonds can resist the water-SiO_2 interactions, thus preventing stripping of asphalt from the aggregate, consistent with practical observation.

Water probably enters the asphalt/siliceous interface by breaking the water-silanol (SiOH) bonds and building up the water layer on the silanol-terminated surface. This occurred because the hydrogen bonds between the first water layer and the silanol groups on a silica surface are substantially weaker (about 25 kJ/mol) than the bonds between the first and second layer of water (>40 kJ/mol) (56).

The contention that the interactions between asphalt/siliceous aggregate bonds are weak and that this weak interaction can not resist water displacement is also strongly supported by a comprehensive analysis by Bolger and Michael (57). They showed that there are only a few organic/substrate combinations, e.g., strong acidic organic/strong basic substrate or strong basic organic/strong acidic substrate, that can resist the displacement by water. The reason for this is mainly that most common metal elements (including Si) are considerably more electropositive than the carbon atoms in organic compounds. Consequently, the electron density on the oxygen atom in the SiO_2 is considerably greater than that on the oxygen in water or in most organic compounds. Therefore, covalently-bonded interfaces are not commonly formed in organic film/unmodified oxide systems, and the secondary-force bonds that do occur are too weak to resist the affinity of water to the polar, high-energy substrate. Thus, if high energy surfaces (e.g. SiO_2) are not modified, water is likely to form a layer at the interface when an organic film/high energy solid is exposed to water or to high relative humidities. This assertion is supported by the well known practice in the polymer/glass fiber composite industry, where the fibers are commonly treated with silane coupling agents to improve the durability of the composites used in moist environments.

The amount of water at the coating/substrate interface is greatly increased if the interface also contains hydrophilic contaminations or an osmotic driving force existing between the interface and the outside. Unfortunately, water soluble inorganic and organic salts are almost ubiquitous contaminants at the asphalt/aggregate interface, either present before the asphalt application or migrating there during service. The effect of hygroscopic contaminants on the thickness of the water adsorbed layer has been discussed in detail in Section 3.3. It should be noted that, in the presence of salt contamination, a liquid phase of water at the interface can be formed at humidities far below the saturation point of water (humidity of liquification). For example, the humidities of liquification of LiCl and $CaCl_2$ are only 15 % and 32 %, respectively (58). Thus, if the interface is contaminated with these salts, it is likely to hold molecular water even at low relative humidities.

The presence of a hydrophilic film at the interface may explain for the differences in thickness of the water layer for different asphalts and between asphalt and epoxy specimens. Asphalts are known to contain water-soluble species, which probably leached out of the film and accumulated

to the interface during exposure. Such a water-sensitive layer at the asphalt/model siliceous interface would result in higher amounts of water entering the interface and greater adhesion loss than those of the epoxy specimens. The presence of a water sensitive layer at the organic film/metal interface has been documented by Walker (55), who found that the concentrations of the water-soluble products accumulated at the coating/substrate interface of the alkyd and epoxy ester coatings were substantially higher than those for the polyurethane coatings. Thus, we believe that there was a layer of hydrophilic materials at the asphalts/SiO_2 interface and this layer was the main reason for the much thicker water layer at the interface for the asphalt specimens than that of the epoxy system. The concentration and nature of this water-sensitive layer were also probably responsible for the different rates and quantities of water at the interface of different SHRP asphalts on the model siliceous substrate.

Water can reach the interface from the outside by a number of pathways, by diffusing through the matrix asphalt and by migrating through pinholes, pores, defects, and local inhomogeneities in the asphalt films. Based on evidence of a large concentration of water present at the interface after a short exposure time and a much thinner water layer for thicker asphalt films, we propose that water transport from the outside to the interface is through water-soluble, hydrophilic regions in an asphalt film. The hydrophilic regions are areas occupied by the highly polar groups of the asphalt molecules or by the water-soluble impurities (e.g., ions and salts) in the asphalt film. It is likely that each water-soluble impurity particle is associated with a polar site in the asphalt. Thus, a hydrophilic region in an asphalt film probably consists of polar groups of the asphalt molecules and water-soluble impurities. This postulation is based on extensive data on the inhomogeneous nature of polymers and on the relationship between polymer heterogeneity and its protective properties (59). Organic polymers are known to consist of high density/high molecular weight segments separated by narrow boundaries of low density/low molecular weight materials. The transport of water through polymer films has been experimentally observed to be not uniform throughout the film surface, but along the boundaries around the high-density, high molecular weight segment (60). The water sorption of the low density/low molecular weight areas has been found to be typical for a hydrophilic, ion-exchange membrane, which usually sorbs 45 % to 75 % water (based on mass) (61). This means that these areas (i.e., the hydrophilic, low density/low molecular weight regions) take up a substantial amount of water and have a much lower ionic resistance than the rest of the film. The corrosion of metals under these polymer coatings has been observed at the locations directly corresponding to the hydrophilic regions (61,62).

We believe that water first dissolves the hydrophilic regions (an emulsification process) and opens up a tortuous pathway system in the asphalt matrix, allowing water containing ions reaching the interface. Thus, the water transport through an asphalt is not a uniform diffusion through the homogeneous asphalt matrix but rather a transport process mediated by the pores, which are opened up by the dissolution by water in the areas occupied by the hydrophilic materials. A similar mechanism has been proposed for the transport of ions through polymer coatings to reach the film/metal interface (59). It is noted that emulsification of straight asphalts is commonly observed and that the emulsified products can dissolve polar as well as nonpolar components of the asphalts. For thick and low water-soluble impurity asphalt film, the pores may not be

continuous from the surface to the interface. In such cases, prolonged or repeated exposure is required for water to reach to the interface. Since the chance for the overlapping of two or more water-soluble regions is small, thicker or multiple layer asphalt film is more effective than a single coat of the same thickness.

The difference between the pore-mediated and homogeneous transports is the stretched exponential decay for the former versus simple exponential decay for the latter (63). The transport increases if there is an osmotic force between the outside environment and the interface, or when the interface also contains hydrophilic contaminants. Once entering the interface, water can transport along the film/substrate interface. For untreated substrate surface, the transport of water along the interface has been found to be much faster than that through a polymer film (64).

In summary, water soluble materials migrated from the environment as well as from the asphalt film, and those present at the interface (from both asphalt and aggregate) constitute a water-sensitive layer at the asphalt/aggregate interface. This water sensitive layer is the main reason for the formation of a water layer many monolayers thick at the interface, responsible for the stripping of asphalt from a siliceous aggregate. Modifying siliceous surface with a monolayer of a base, such as an amine, will render the surface basic. This surface would form strong bonds with the acidic asphalts and thus can resist the water displacement.

5. IMPACT ON HIGHWAY TECHNOLOGY

Besides measuring in-situ water at the asphalt/siliceous aggregate interface, the developed FTIR technique can provide a method for:

1. Evaluating the water susceptibility of different asphalt binders on a siliceous aggregate,
2. Evaluating and screening antistripping agents for asphalts on a siliceous aggregate. (Antistripping agents may be mixed in the asphalt binders or applied on siliceous aggregate surface before hot mixing.)
3. Conveniently investigating the effects of aggregate surface contamination, hot mix temperatures, and service conditions on the water stripping of asphalt on a siliceous aggregate.
4. Measuring the diffusion of water through a layer of asphalt to a siliceous surface (essential for stripping modeling).
5. Measuring *in situ* organic and inorganic compounds at the asphalt/aggregate interface.
6. Measuring transport properties of water, organic, and inorganic materials through a layer of asphalt/aggregate mixture or concrete on a substrate.

6. CONCLUSIONS

A sensitive, spectroscopic technique for measuring water *in situ* at the asphalt/model siliceous aggregate has been developed. The technique can detect and also provide quantitative information on the water at the asphalt/siliceous aggregate interface. This information, which relates to the

adhesion loss of asphalt/siliceous aggregate mixture, will be useful for predicting the water susceptibility of asphalt/siliceous aggregate mixtures. The technique is convenient for studying the effects of the aggregate, contamination of the aggregate, antistripping agents, and the asphalt, on the water susceptibility of asphalt/siliceous aggregate mixtures. It is also unique in providing data on the transport of water through an asphalt layer of any thickness attached to an aggregate. It is anticipated that the technique will have a wide range of applications in highway technology. In addition to the spectroscopic technique, the adhesion test method developed in this study would also provide a useful tool for conveniently evaluating, both in the field and in the laboratory, the effectiveness of antistripping agents and the relative water stripping resistance of different asphalts on a flat substrate.

7. ACKNOWLEDGMENTS

8. REFERENCES

1   P. Hubbard, Adhesion of Asphalt to Aggregate in the Presence of Water, Proceedings, **Highway Research Board**, 1938, Vol. 18, Part I, p. 238.

2   K. Majidzadeh and F. N. Brovold, State of the Art: Effect of Water on Bitumen-Aggregate Mixtures, **Highway Research Board**, Special Report 98, 1968, pp 1-62.

3   M. A. Taylor and N. P. Khosla, Stripping of Asphalt Pavements: State of the Art, **Transportation Research Record** 911, 1983, p. 150.

4   A. J. Kinloch, in **Durability of Structural Adhesives**, A. J. Kinloch, Ed., Applied Science Publishers, New York, 1983, pp. 1-39.

5   A. C. Zettlemoyer, F. J. Micale, and K. Klier, in **Water, A Comprehensive Treatise**, F. Franks, Ed., Plenum Press, N. Y., 1975, Vol.5, Chapter 5.

6   L.H. Little, **Infrared Spectra of Adsorbed Species**, Academic Press, N.Y., 1966.

7   P.A. Thiel and T.E. Madey, **Surface Sci. Rep.**, 7 (1987) 211.

8   K. Ashley and S. Pons, **Chem. Rev.**, 88 (1988) 673.

9   R. Miles, **Surface Interface Anal.**, 5 (1983) 43.

10   J. N. Israelachvili, **J. Colloid Interface Sci.**, 110 (1986) 263.

11   R. G. Horn, D. T. Smith, and W. Haller, **Chem. Phys. Lett.**, 162 (1989) 404.

12   N.J. Harrick, **J. Opt. Soc. Am.**, 55 (1965) 851.

13   N.J. Harrick, **Internal Reflection Spectroscopy**, Harrick Sci., Ossining, N.Y., 1979.

14   F.M. Mirabella, **Appl. Spectrosc. Revs.**, 21 (1985) 95.

15   F.M. Mirabella, **Spectrosc.**, 5 (1990) 20.

16   R. Iwamoto and K. Ohta, **Appl. Spectrosc.**, 38 (1984) 359.

17   K. Ohta and R. Iwamoto, **Appl. Spectrosc.**, 39 (1985) 418.

18   R.J. Jakobsen, in J.R. Ferraro and L.J. Basile (eds.) **Fourier Transform Infrared Spectroscopy - Applications to Chemical Systems**, Academic Press, N.Y., 1979, Vol. 2, p. 165.

19   V.M. Zolotarev, V.I. Lygin, and B.N. Tarasevich, **Russian Chemical Reviews, 50** (1981) 14.

20   T. Nguyen, T., **Prog. Organic Coatings.**, 13 (1985) 1.

21   H. Ishida, **Rubber Chem. Technol.**, 60 (1987) 498.

22   J. Yardwood, **Spectrosc.**, 5 (1990) 35.

23   Y. Ozaki, Y. Fujimoto, S. Terashita, and N. Katayama, **Spectrosc.**, 8 (1993) 36.

24   T. Nguyen, E. Byrd and D. Bentz, National Institute of Standards and Technology Internal Report, Internal Report No. NISTIR 4783, March, 1992.

25   T. Nguyen, D. Bentz, and W.E. Byrd, **J. Coatings Technol.**, 66, No. 834 (1994) 39.

26   G. Muller, D.K. Abraham, and M. Schaldach, **Appl. Optics**, 20 (1981) 1182.

27   J. F. Branthaver, J. C. Peterson, J. J. Duvall and P. M. Harnsberger, Investigation of Compatibilities of SHRP Asphalts, Paper presented at the **TRB Annual Meeting**, Washington, D.C., January, 1991.

28   R.K.Iler, **The Chemistry of Silica**, John Wiley and Sons, N.Y., 1979, Chapter 6, p. 627.

29   T. Nguyen, W. E. Byrd, and D. Bentz, **J. Adhesion**, 48 (1995) 169.

30   T. Nguyen, D. Bentz, E. Byrd, and C. Lin, **Prog. Organic Coatings**, 27 (1996) 181.

31   T. Nguyen, W.E. Byrd, D. Alsheh, W. McDonough, and J. Seiler, Proc., **Materials Research Society Meeting**, April, 1995.

32   For a brief review on this subject, see C.L. Schutte, **Materials Sci. and Eng.**, R13 (1994) 265.

33.   G. Abson and C. Burton, Physical Tests and Range of Properties, in **Bituminous Materials: Asphalts, Tars, and Pitches, Vol. 1: General Aspects**, A. J. Holberg, Ed., Robert E. Krieger Publishing Company, N.Y., 1979, pp 213-288.

34   T. Nguyen, D. Bentz, and W.E. Byrd, **J. Coatings Technol.**, 67, No. 844 (1995) 37.

35   R.U. Dietuich and J. T. Putro, Jr.(Eds), AGI data Sheets, **Am. Geological Institute**, 1982, p.44.1.

36   T.D. Taylor, in **Engineering Materials Handbook: Ceramics and Glasses**, ASM International, 1991, p. 566.

37   ASTM D 4541-1995, Pull off Strength of Coatings Using Portable Adhesion Tester, Annual Book of ASTM Standards, Vol. 06.01, 1995, American Society for Testing and Materials, Philadelphia, PA.

38   L. Holland, **The Properties of Glass Surfaces**, Wiley, N.Y. 1964, p. 180.

39   R.G. Pike and D. Hubbard, **J. Res. Nat. Bur. Stand.**, 59 (1957) 127.

40   V.R. Deitz, Naval Research Laboratory NRL Report 6812, Washington D.C., 1968.

41.   F. P. Bowden and W. R.Throssell, **Pro. Royal Soc.**, 209 (1951) 297.

42   J. C.Frazer, W.A. Patrick, and H.E.Smith, **J. Phys. Chem.**, 31 (1927) 897.

43.   J. W. Healy and D.W. Fuerstenau, **J. Colloid Sci.**, 20 (1965) 376.

44.   F.M. Fowkes, in **Physicochemical Aspects of Polymer Surfaces**, K.L. Mittal (Ed.), Plenum Press, N.Y. , 1983, p. 583.

45   C. W. Curtis, K. Ensley, and J. Epps, SHRP A-003B, Fundamental Properties of Asphalt/Aggregate Interactions Including Adhesion and Absorption, **Strategic Highway Research Program**, National Research Council, Washington, D.C., Final Report, August,

1991.

46   H. Leidheiser, Jr. and W. Funke, **J. Oil and Color Chemists' Assoc.** 5 (1987) 121.

47   T. Nguyen, W.E. Byrd, D. Alsheh, and D. Bentz, Proc., **Adhesion Society Meeting,** February, 1995, p 252.

48   E. McCafferty, V. Pravdic and A.C. Zettlemoyer, **Tran. Faraday Soc.,** 66 (1979) 1720.

49   F.J. Micale, M. Topic, H. Leidheiser and A.C. Zettlemoyer, **J. Colloid Interface Sci.,** 55 (1976) 540.

50   F. P. Bowden and W. R.Throssell, **Nature,** 167 (1957) 601.

51   J.W. Debye and K.H. van Beek, **J. Chem. Phys.,** 31 (1959) 1595.

52.   W. D. Bascom, **J. Adhesion,** 2 (1970) 168.

53   A.J. Kinloch (Ed.), **Durability of Structural Adhesives,** Applied Sci., N.Y., 1983.

54.   K. L. Mittal (Ed.), **Adhesion Aspects of Polymeric Coatings,** Plenum Press, N.Y., 1983, Part III: Bond Durability.

55   P. Walker, **Official Digest,** 12 (1965) 1561 ; **J. Paint Technol.,** 31 (1967) 22.

56   K. Klier and A.C. Zettlemoyer, **J. Colloid Interface Sci.,** 58 (1977) 216.

57   J.C. Bolger and A.S. Michaels, in P. Weiss and D. Deevers (Eds.) **Interface Conversion for Polymer Coatings,** Elsevier, N.Y., 1969, p. 3.

58   W. Funke, **Prog. Organic Coatings,** 9 (1981) 29.

59   For a brief review on this subject see T. Nguyen, J.B. Hubbard, and J.M. Pommersheim, **J. Coatings Technol.,** 68, no. 855 (1996).

60   M.I. Karyakina and A.E. Kuzmak, **Prog. Organic Coatings,** 18 (1990) 325.

61   R. Fernandez-Prizi and H. Corti, **Prog. Organic Coatings,** 10 (1982) 5.

62   D.J. Mills and J.E.O Mayne, in **Corrosion Control by Organic Coatings,** H. Leidheiser (Ed.), National Association of Corrosion Engineers, Houston, TX, 1981, p. 12.

63   J. B. Hubbard, T. Nguyen, and D. Bentz, **J. Chem. Phys.,** 96 (1992) 3177.

64.   Linossier, I., Gaillard, F., and Romand, M., Proc., **Adhesion Society Meeting,** February, 1995, p. 86.